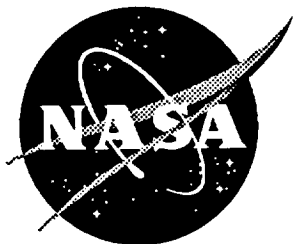


IN-15
45762
P 69

NASA Technical Memorandum 110155



(NASA-TM-110155) EFFICIENT
EIGENVALUE ASSIGNMENT BY STATE AND
OUTPUT FEEDBACK WITH APPLICATIONS
FOR LARGE SPACE STRUCTURES (NASA,
Langley Research Center) 69 p

N95-24581

Unclass

G3/18 0045762

Efficient Eigenvalue Assignment by State and Output Feedback with Applications for Large Space Structures

Eric C. Vannell
*George Washington University
Joint Institute for the Advancement of Flight Sciences
Langley Research Center, Hampton, Virginia*

Sean P. Kenny
Langley Research Center, Hampton, Virginia

Peiman G. Maghami
Langley Research Center, Hampton, Virginia

March 1995

National Aeronautics and
Space Administration
Langley Research Center
Hampton, Virginia 23681-0001

— —

Abstract

The erection and deployment of large flexible structures having thousands of degrees of freedom require controllers based on new techniques of eigenvalue assignment that are computationally stable and more efficient. Scientists at NASA Langley Research Center have developed a novel and efficient algorithm for the eigenvalue assignment of large, time-invariant systems using full-state and output feedback. The objectives of this research were to improve upon the output feedback version of this algorithm, to produce a toolbox of MATLAB functions based on the efficient eigenvalue assignment algorithm, and to experimentally verify the algorithm and software by implementing controllers designed using the MATLAB toolbox on the Phase 2 configuration of NASA Langley's Controls-Structures Interaction Evolutionary Model, a laboratory model used to study space structures. Results from laboratory tests and computer simulations show that effective controllers can be designed using software based on the efficient eigenvalue assignment algorithm.

Table of Contents

	Page
Abstract	i
List of Tables	v
List of Figures	vi
1. INTRODUCTION	1
1.1. Literature Survey	1
1.1.1 Strict Eigenvalue Assignment	3
1.1.2 Eigenstructure Assignment	6
1.2. Research Objective	7
1.3. Outline	8
2. EFFICIENT EIGENVALUE ASSIGNMENT	9
2.1. Full-State Feedback	9
2.1.1 Theory	9
2.1.2 Sample Problem with Full-State Feedback	16
2.2. Output Feedback	20
2.2.1 Theory	20
2.2.2 Optimized Output Feedback	25
3. IMPLEMENTATION OF STATE FEEDBACK EFFICIENT EIGENVALUE ASSIGNMENT CONTROLLER ON PHASE 2 CEM	28
3.1. Phase 2 CEM Description	28
3.2. Modeling of Phase 2 CEM	29
3.3. Controller Design and Phase 2 CEM Implementation	32

3.4. Test Procedure and Results	35
3.5. Discussion of Results	44
4. SIMULATION OF OPTIMIZED OUTPUT FEEDBACK EFFICIENT EIGENVALUE ASSIGNMENT CONTROLLER ON PHASE 2 CEM . . .	51
4.1. Controller Design	51
4.2. Simulation Results	52
5. CONCLUSIONS	57
References	59

List of Tables

Table		Page
1	Phase 2 CEM – Measured Open-Loop Modal Information	34
2	Phase 2 CEM – Performance of EEA Controller	36
3	Phase 2 CEM – Measured and Modeled Open-Loop Modes of Vibration . . .	44
4	Phase 2 CEM – Effect of Modeling Errors on Desired Damping using State Feedback	46
5	Optimized Output Feedback: Open-Loop and Closed-Loop Eigenvalues . . .	53

List of Figures

Figure	Page
1 Flowchart of State Feedback EEA Algorithm	15
2 Spring-Mass-Damper System	16
3 Flowchart of Optimized Output Feedback EEA Algorithm	27
4 CSI Evolutionary Model - Phase 2	29
5 State Feedback Test 2: Closed-Loop versus Open-Loop Time Response . . .	38
6 State Feedback Test 6: Closed-Loop versus Open-Loop Time Response . . .	39
7 State Feedback Test 9: Closed-Loop versus Open-Loop Time Response . . .	40
8 State Feedback Test 11: Closed-Loop versus Open-Loop Time Response . . .	41
9 State Feedback Test 13: Closed-Loop versus Open-Loop Time Response (Accelerometer/Thruster Pairs 1&5)	42
10 State Feedback Test 13: Closed-Loop versus Open-Loop Time Response (Accelerometer/Thruster Pairs 8&4)	43
11 40 Second Open-Loop Out-of-Phase Excitation of Phase 2 CEM	47
12 10 Second Open-Loop Excitation of Phase 2 CEM at Correct Natural Frequencies	47
13 Time Response Comparison of Phase 2 CEM Test 1 with MATLAB Simulation of Test 1	49
14 Time Response Comparison of Phase 2 CEM Test 11 with MATLAB Simulation of Test 11	50
15 Output Feedback Simulation: Closed-Loop 1% Damping versus Open-Loop Time Response	55
16 Output Feedback Simulation: Closed-Loop 4% Damping versus Open-Loop Time Response	55

17	Output Feedback Simulation: Closed-Loop 10% Damping versus Open-Loop Time Response	56
----	---	----

1. INTRODUCTION

1.1. Literature Survey

One of the widely used methods of modifying the dynamic response of a linear time-invariant system is the placement of the closed-loop eigenvalues at prescribed locations in the complex plane via linear state or output feedback. Since Wonham [1] established the relationship between the controllability of linear multivariable systems and the assignability of the eigenvalues by full-state feedback, this problem has received considerable attention. The problem was expanded to the simultaneous assignment of eigenvalues and eigenvectors after Moore [2] showed the nonuniqueness of control gains (or eigenvectors) for the placing of eigenvalues, and characterized the class of all closed-loop eigenvector sets attainable for a given set of closed-loop eigenvalues. The area of research has also been extended to consider the output feedback problem, because in most practical situations the full states are not directly available. The limitations imposed by output feedback were established by Davison and Wang [3], Srinathkumar [4], and others. This section will review and compare some of the existing literature in the field of eigenvalue and eigenvector assignment by state and output feedback.

Linear, time-invariant, multi-input/multi-output (MIMO) systems can be represented by equations of the form:

$$\dot{\mathbf{x}}(t) = A\mathbf{x}(t) + B\mathbf{u}(t) \quad (1.1)$$

$$\mathbf{y}(t) = C\mathbf{x}(t) \quad (1.2)$$

where A is an $n \times n$ state matrix, B is an $n \times m$ control input influence matrix, C is a $p \times n$ output influence matrix, $\mathbf{x}(t)$ is an $n \times 1$ state vector, $\mathbf{y}(t)$ is a $p \times 1$ output measurement vector, and $\mathbf{u}(t)$ is an $m \times 1$ control input vector. In all cases the system is assumed to be

completely controllable, and in the case of output feedback, completely controllable and observable. Controllability measures the particular actuator input configuration's ability to control all system states, whereas observability measures the particular sensor output configuration's ability to obtain the information needed to estimate all system states. The following are the formal definitions of these concepts for linear systems defined by Eqs. (1.1) and (1.2).

A linear system is said to be completely controllable if for any initial time t_0 , there exists a set of unconstrained controls $u(t)$, that will transfer each initial state $x(t_0)$ to any final state $x(t_1)$ in some finite time $t_1 > t_0$. A linear system is said to be completely observable if at any initial time t_0 , the initial state $x(t_0)$ can be determined from the knowledge of the output $y(t)$ and the input $u(t)$ for times $t_0 \leq t \leq t_1$, where t_1 is some finite time [5].

The eigenvalue assignment problem for full-state feedback entails finding an $m \times n$ constant state feedback matrix G , used in the control law

$$u(t) = -Gx(t)$$

such that the resulting closed-loop state matrix,

$$\hat{A} = A - BG$$

has all eigenvalues at desired locations in the complex plane. The associated problem for output feedback has a controller of the form

$$u(t) = -Gy(t)$$

and G must be chosen to produce the desired eigenvalues of the resulting closed-loop state matrix

$$\hat{A} = A - BGC$$

The existing state and output feedback control methods can be classified into two categories: strict eigenvalue assignment and eigenstructure assignment. The strict eigenvalue assignment approach deals with modifying a system's behavior strictly through the placement of the closed-loop eigenvalues. The nonunique solutions for multi-input systems, as detailed by Moore [2], are addressed by these approaches either by presenting the set of solutions that can be obtained, or by constraining the solution to maximize a performance measure, i.e., a measure of closed-loop system robustness or some norm of the gain matrix. Robustness is a measure of the insensitivity of the closed-loop eigenvalues to system perturbations. Eigenstructure assignment is the simultaneous assignment of the eigenvalues and eigenvectors. The assigned eigenvalues affect the speed of response of the closed-loop system, whereas the eigenvectors affect the relative shape of the transient response. Some of these approaches also seek to minimize certain measures of the closed-loop system. It should be noted that for the sake of completeness, both eigenvalue assignment and eigenstructure assignment techniques are reviewed in this paper. Although this paper reviews both eigen-assignment techniques, it focuses primarily on eigenvalue assignment techniques.

1.1.1 Strict Eigenvalue Assignment

In the past decade many algorithms for strict eigenvalue assignment have utilized some triangular form of the closed-loop system matrix. One such form is the real Schur form [6], which is generated by an orthogonal similarity transformation that yields a quasi-upper triangular matrix, having only 1×1 or 2×2 blocks on the diagonal corresponding to real or to complex conjugate eigenvalues, respectively. Varga [7] proposed a state feedback, pole-shifting procedure that modifies only the unstable eigenvalues of the system. This partial eigenvalue assignment method is based on the Schur form of the state matrix and on the use of QR decomposition [6]. The poles that are chosen to be

assigned are moved down the main diagonal of the state matrix using QR decomposition and are assigned sequentially. Meanwhile, the resulting gains in the feedback matrix are minimized. Later this procedure was the basis for the method of Maghami and Juang [8] which uses the complex Schur form along with unitary coordinate transformations, or Givens rotations [6], instead of QR decomposition to move the eigenvalues down the main diagonal. A similar procedure for eigenvalue assignment was also developed in [8] using output feedback. Petkov, et al. [9], [10] presented an algorithm which also makes use of the Schur form and provides numerical stability, which makes it applicable to ill-conditioned and high-order problems. This method is professed to perform equally well with real and complex, distinct, and multiple desired poles. However, the procedure does not seek to enhance the robustness nor minimize the resulting gains.

Patel and Misra [11], [12] proposed algorithms for eigenvalue assignment which deal with the systems in upper Hessenberg form (UHF) [6]. A matrix H is said to be in upper Hessenberg form if the elements $h_{ij} = 0$, $i > j + 1$. UHF can be achieved through a series of Householder transformations [6]. Patel and Misra's first group of algorithms [11] use state feedback to solve the assignment problem for multi-input systems. The multi-input systems are reduced to one or more single-input systems where the single-input systems are in UHF. A type of QR algorithm is then used to solve the eigenvalue assignment problem for the individual single-input systems. A similar procedure is described in [12] for output feedback. In both papers the procedures assign all of the system's eigenvalues, and no consideration is given to the robustness of the system.

Datta [13] also proposed an algorithm for state feedback eigenvalue assignment using the UHF of the system equations. However, this algorithm only solves the assignment problem for single-input systems. Later Arnold and Datta [14] extended this approach to multi-input systems. Their algorithm does not make use of a QR type

method, but instead uses a simple linear recursion. Although this algorithm is not a robust pole placement algorithm, the authors claim that it gives comparable results in “well-conditioned” problems with fewer computations.

In the literature there are several iterative approaches that directly exploit the freedom offered by the multi-input multi-output eigenvalue assignment problem to improve the performance of the closed-loop system or to minimize the required control effort. One such algorithm was presented by Kautsky et al [15]. Kautsky’s algorithm iteratively maximizes a robustness measure of the closed-loop system in terms of the conditioning of the closed-loop modal matrix through an orthogonal projection approach. This method requires the assignment of all the eigenvalues of the system and works only for full-state feedback.

It is also to be noted that there exist methods in which the eigenvalue placement constraints are in the form of Sylvester’s equation [16], [17]. The assignment is done via state feedback, where the feedback gain, G , is calculated by solving the matrix equations

$$AT - T\hat{A} = -BP \quad (1.3)$$

$$GT = P \quad (1.4)$$

for a fixed closed-loop matrix, \hat{A} , subject to a parameter matrix chosen such that (\hat{A}, P) is observable. Equation. (1.3) is referred to as Sylvester’s equation. For this method \hat{A} is chosen to have all the desired closed-loop eigenvalues. Then P is picked arbitrarily, based on the criteria described above, and Eq. (1.3) is solved for a nonsingular matrix T . Finally, Eq. (1.4) is solved for G , i.e. $G = PT^{-1}$. These methods based on Sylvester’s equation work only for full assignment of distinct eigenvalues.

1.1.2 Eigenstructure Assignment

Moore [2] identified the flexibility beyond strict eigenvalue assignment for multi-input systems by characterizing the attainable eigenvector space for a set of desired closed-loop eigenvalues. It was shown that in addition to specifying the closed-loop eigenvalues, one has a freedom to choose one set of closed-loop eigenvectors from this attainable space. This result opened the door for research into eigenstructure assignment. Fahmy and O'Reilly [18], [19] parameterized the set of associated eigenvectors and generalized eigenvectors and presented a state feedback eigenstructure assignment algorithm. Tsui [20] provided a method that deals with the system in upper Hessenberg form. This state feedback approach supplies a way to reduce the condition number of the final modal matrix resulting in better transient response and robustness. This method can assign both distinct and multiple eigenvalues. Kwon and Youn [21] lifted some of the restrictions on previous eigenstructure assignment techniques in an algorithm that uses output feedback. Their method allows for closed-loop eigenvalues that need not be distinct or different from the eigenvalues of the open-loop system.

In the area of robust eigenstructure assignment, Juang et al. [22] developed a method in which the closed-loop eigenvectors are chosen to maximize the projection on the open-loop eigenvectors or the columns of the closest unitary matrix to the open-loop eigenvector matrix, in order to obtain a robust closed-loop design. This approach was later extended to provide robust eigenstructure assignment for second order dynamic systems [23], and then for state estimators using second order models [24].

Other methods of eigenstructure assignment have also been proposed. Maghami et al. [25] uses a subspace intersection technique to assign closed-loop eigenvalues via output feedback. It represents an extension of [22] by allowing the assignment of the maximum possible number of closed-loop eigenvalues. Lu et al. [26] developed partial

eigenstructure assignment, where the shape of the transient response corresponding to the unchanged eigenvalues is controlled by prespecifying the closed-loop eigenvectors associated with the unchanged eigenvalues before assigning the modified eigenvalues along with the eigenvectors. This algorithm was shown to be effective for large scale system applications. Eigenstructure assignment employing output feedback was also shown to be possible using Sylvester's equation, as was illustrated in [27].

1.2. Research Objective

Traditionally, eigenvalue assignment algorithms have been used as control design tools for linear time-invariant systems. Conventional eigenvalue assignment methods require that all eigenvalues be assigned to specified locations. Controller design for large order systems using conventional assignment methods proves to be computationally excessive because of the large number of eigenvalues that must be assigned. Eigenvalue assignment algorithms which utilize partial assignment of eigenvalues, i.e., only a small subset of all eigenvalues are placed, provides the computational efficiency needed for large order systems. Future space missions that will utilize large flexible structures can directly benefit from control design tools developed from these principles.

The objectives of this research are to:

1. Program controller design software based on the Efficient Eigenvalue Assignment (EEA) algorithms for full-state and output feedback of Maghami and Juang [8].
2. Develop and program a new output feedback EEA algorithm to obtain a stable closed-loop system.
3. Experimentally verify the controller design software as well as the methods themselves by implementing several EEA controllers on Phase 2 of NASA Langley Research Center's Controls-Structures Interaction (CSI) Evolutionary Model.

The EEA algorithms will be programmed in MATLAB [28] language and expressed in M-files. This collection of files will be named the MATLAB EEA Toolbox. The new output feedback EEA algorithm will be an extension to the original output feedback algorithm and will use optimization to produce an output feedback gain matrix that will provide eigenvalue assignment while guaranteeing closed-loop stability.

1.3. Outline

The paper is divided into three main parts. First, Chapter 2 will present the theory behind the EEA algorithm of Maghami and Juang [8]. It will detail the full-state feedback method of eigenvalue assignment and illustrate the use of the method in a sample problem. The output feedback method will also be discussed in Chapter 2, and a new method of optimized output feedback to guarantee closed-loop stability will be proposed.

Chapter 3 will deal with the implementation of controllers designed using the state feedback EEA algorithm on the Phase 2 configuration of the CSI Evolutionary Model, a simulated space structure laboratory testbed. A discussion will be given on the controller design software and the test procedures used. Closed-loop modal parameters and time response data from the tests will be presented to experimentally verify the controller design software and the EEA algorithm.

Chapter 4 will describe the controller design software produced from the new optimized output feedback EEA algorithm. Computer simulations of closed-loop systems consisting of a Phase 2 mathematical model and controllers designed using optimized output feedback will be presented. Simulated closed-loop modal parameters and time response data will be supplied for verification of the algorithm and software.

Finally, Chapter 5 will provide a brief summary of the material presented in this work. Also, a suggestion for future research is provided.

2. EFFICIENT EIGENVALUE ASSIGNMENT

The control method implemented in this study was the EEA algorithm as described by Maghami and Juang [8]. Eigenvalue assignment, via state or output feedback, is a commonly used method of modifying the dynamic response of a linear time-invariant system. While most algorithms of this nature attempt to assign all the eigenvalues of the system, Maghami and Juang's algorithm attains efficiency by sequentially assigning one eigenvalue at a time without shifting the remaining eigenvalues. This approach is especially efficient when the number of assigned eigenvalues is less than the order of the system. This is particularly true for the control of large space structures which have thousands of degrees of freedom.

2.1. Full-State Feedback

2.1.1 Theory

The full-state feedback approach for this algorithm basically consists of three steps. First, a Schur decomposition is applied to triangularize the state matrix. Second, a series of coordinate rotations (Givens rotations) are used to move the eigenvalue to be assigned to the end of the diagonal of the Schur form. Third, the eigenvalue is assigned to a desired location by full-state feedback without affecting the remaining eigenvalues. The second and third steps are repeated until all the requested eigenvalues are moved to the desired locations. Given the freedom of multiple inputs, the feedback gain matrix is calculated to minimize an objective function composed of the Frobenius norm of the gain matrix. The Frobenius norm of a matrix is the root sum squared of the elements of the matrix.

Once again considering the linear system defined by Eq. (1.1) and (1.2) which is assumed to be completely controllable. Full-state feedback is used to design a constant

feedback controller with a gain matrix G_1 of dimension $m \times n$, such that $u(t) = G_1 x(t)$. The gain matrix G_1 is to be chosen in such a way that either a real eigenvalue or a complex conjugate pair of eigenvalues of the open-loop state matrix A are assigned to desired values without shifting the remaining eigenvalues.

The eigenvalue assignment method for full-state feedback starts with applying the Schur transformation to Eq. (1.1), i.e.,

$$\mathbf{x} = V\mathbf{x}_1 \quad (2.1)$$

and premultiplying the resulting equation by V^H to yield

$$\dot{\mathbf{x}}_1 = V^H A V \mathbf{x}_1 + V^H B G_1 V \mathbf{x}_1 \quad (2.2)$$

where V is an $n \times n$ unitary Schur matrix and $(\)^H$ denotes the complex conjugate transpose. The state matrix in the transformed coordinates, namely, $V^H A V$ is an upper triangular matrix with the eigenvalues of A on the diagonal, i.e.,

$$V^H A V = \begin{bmatrix} \lambda_1 & \mathcal{X}_{12} & \cdots & \mathcal{X}_{1n} \\ 0 & \lambda_2 & \cdots & \mathcal{X}_{2n} \\ \vdots & \vdots & \ddots & \vdots \\ 0 & 0 & \cdots & \lambda_n \end{bmatrix}$$

where \mathcal{X}_{ij} denotes the matrix elements above the diagonal. Observe from Eq. (2.2) that it is possible to derive a gain matrix $G_1 V$ (in the transformed coordinates) such that the feedback portion of the closed-loop state matrix, namely, $V^H B G_1 V$, is an upper triangular matrix with all diagonal elements zero except the last. Hence, with such a gain matrix, the last eigenvalue of matrix A (the last element on the diagonal of $V^H A V$) can be assigned to a desired value without shifting the remaining eigenvalues of A . In order to extend this technique to assign any arbitrary eigenvalue λ_i (the i th value on the diagonal of $V^H A V$), a series of appropriate coordinate transformations (coordinate system rotations) must be used to move λ_i to the last position on the diagonal. This

is accomplished with a unitary Givens rotation, R_i , applied such that $\mathbf{x}_1 = R_i \mathbf{x}_{R_i}$. The form of the Givens rotation matrix is

$$R_i = \begin{bmatrix} 1 & 0 & \cdots & & \cdots & 0 \\ 0 & 1 & 0 & & & \vdots \\ \vdots & & \ddots & & & \\ & & & c_i & s_i^* & \\ & & & -s_i & c_i & \vdots \\ \vdots & & & & & \ddots & 0 \\ 0 & \cdots & & \cdots & 0 & 1 \end{bmatrix} \quad (2.3)$$

where c_i and s_i are, respectively, real and complex scalar parameters defined such that

$$c_i^2 + s_i s_i^* = 1 \quad (2.4)$$

and the superscript * denotes the complex conjugate. The required parameters c_i and s_i of Eq. (2.3) are determined from

$$c_i^2 = \frac{bb^*}{bb^* + (\lambda_i - \lambda_{i+1})(\lambda_i - \lambda_{i+1})^*} \quad (2.5)$$

$$s_i = \frac{(\lambda_i - \lambda_{i+1})c_i}{b} \quad (2.6)$$

where b is the $(i, i+1)$ element of the matrix $V^H AV$. Note that if $b = 0$, then c_i and s_i are, respectively, set to 0 and 1 in Eq. (2.3).

The result of the coordinate transformation is to switch the positions of λ_i and λ_{i+1} on the diagonal. The state matrix in the transformed coordinates thus becomes

$$R_i^H V^H AV R_i = \begin{bmatrix} \lambda_1 & \mathcal{X}_{12} & \cdots & \cdots & \mathcal{X}_{1n} \\ 0 & \ddots & & & \mathcal{X}_{2n} \\ \vdots & & \lambda_{i+1} & & \vdots \\ & & & \lambda_i & \\ \vdots & & & & \ddots & \vdots \\ 0 & 0 & \cdots & \cdots & \lambda_n \end{bmatrix} \quad (2.7)$$

This transformation is repeated $n-i$ times in order to move λ_i to the last position on the diagonal. The dynamics of the system in the final transformed coordinates may be written as

$$\dot{\mathbf{x}}_2 = L^H AL \mathbf{x}_2 + L^H B G_1 L \mathbf{x}_2 \quad (2.8)$$

or

$$\dot{\mathbf{x}}_2 = \bar{A}\mathbf{x}_2 + \bar{B}\bar{G}_1\mathbf{x}_2 \quad (2.9)$$

where L is the composite unitary transformation that moves λ_i to the end of the diagonal and is given as follows:

$$L = VR_iR_{i+1}R_{n-i} \quad (2.10)$$

and

$$\bar{A} = L^H AL; \quad \bar{B} = L^H B; \quad \bar{G}_1 = G_1 L \quad (2.11)$$

To ensure the assignment of the desired value for λ_i , without affecting the remaining eigenvalues, the matrix \bar{G}_1 is chosen in such a way that $\bar{B}\bar{G}_1$ is an upper triangular matrix with diagonal elements zero except for the last element. Such a gain matrix may be of the form

$$\bar{G}_1 = (0 \mid \bar{\mathbf{g}}_1) \quad (2.12)$$

where $\bar{\mathbf{g}}_1$ is an $m \times 1$ vector. Obviously, with such a choice, $\bar{B}\bar{G}_1$ would be a null matrix except for the last column. The local gain matrix G_1 is related to the vector $\bar{\mathbf{g}}_1$ from Eq. (2.11)

$$G_1 = \bar{\mathbf{g}}_1 L_n^H \quad (2.13)$$

where L_n represents the last column of the transformation matrix L .

Assuming that μ_i is the desired closed-loop value for λ_i , then $\bar{\mathbf{g}}_1$ is determined such that

$$b_n \bar{\mathbf{g}}_1 = \mu_i - \lambda_i \quad (2.14)$$

in which b_n represents the last row of the current matrix \bar{B} . Any given solution of $\bar{\mathbf{g}}_1$ that satisfies Eq. (2.14) will then produce a local gain matrix G_1 from Eq. (2.13) that will

move the eigenvalue λ_i to the desired eigenvalue μ_i . Now, depending on the number of control inputs, an optimum solution for \bar{g}_1 corresponding to a minimum gain design may be formulated.

The vector \bar{g}_1 is chosen to minimize a cost function that includes the current global gain matrix, which is obtained by adding all the local gain matrices that assign all the eigenvalues $\lambda_j, j = 1, \dots, i-1$ to the desired eigenvalues $\mu_j, j = 1, \dots, i-1$, and keep the remaining eigenvalues unchanged. This cost function along with the constraint of Eq. (2.14) represents an optimization problem. The optimal solution yields a gain matrix that would assign the i th eigenvalue λ_i to a desired value μ_i , keep the other eigenvalues of the current state matrix unchanged, and minimize the Frobenius norm of the global gain matrix. The Frobenius norm for the global gain matrix, G , is calculated by taking the square root of the sum of the diagonal components of $(G^T G)$. The choice of the cost function to minimize the norm of the gain matrix is particularly practical for applications where available control power is limited.

Using Lagrangian multipliers [29], the optimization problem can be reduced to the solution of a system of simultaneous equations. Once the solution for the local gain matrix is obtained, it is added to the global gain matrix to produce the new global gain matrix, i.e. $G \equiv G + G_1$. The state matrix \bar{A} is similarly updated

$$\bar{A} \equiv \bar{A} + \bar{B}\bar{G}_1 \quad (2.15)$$

Obviously, any practical solution for the local gain matrix must be real, but the solution of the optimization problem is, in general, complex. This problem is overcome by adding an additional constraint to the optimization problem to ensure that the global gain matrix is real when the complex conjugate of the eigenvalue λ_i , namely λ_i^* , is being assigned. First a series of Givens rotations are employed to move λ_i^* to the end

of the diagonal. Then the required gain matrix is determined from the solution to the second optimization problem. Afterwards, the global gain matrix and the state matrix are once again updated. This solution provides a second local gain matrix that assigns the eigenvalue λ_i^* to the desired value μ_i^* . In the case where the eigenvalue to be assigned is real, this second optimization is not necessary. This entire procedure of Givens rotations and optimized assignment by full-state feedback is repeated until all the requested eigenvalues are assigned to the desired locations. Figure 1 shows the details of the entire eigenvalue assignment algorithm.

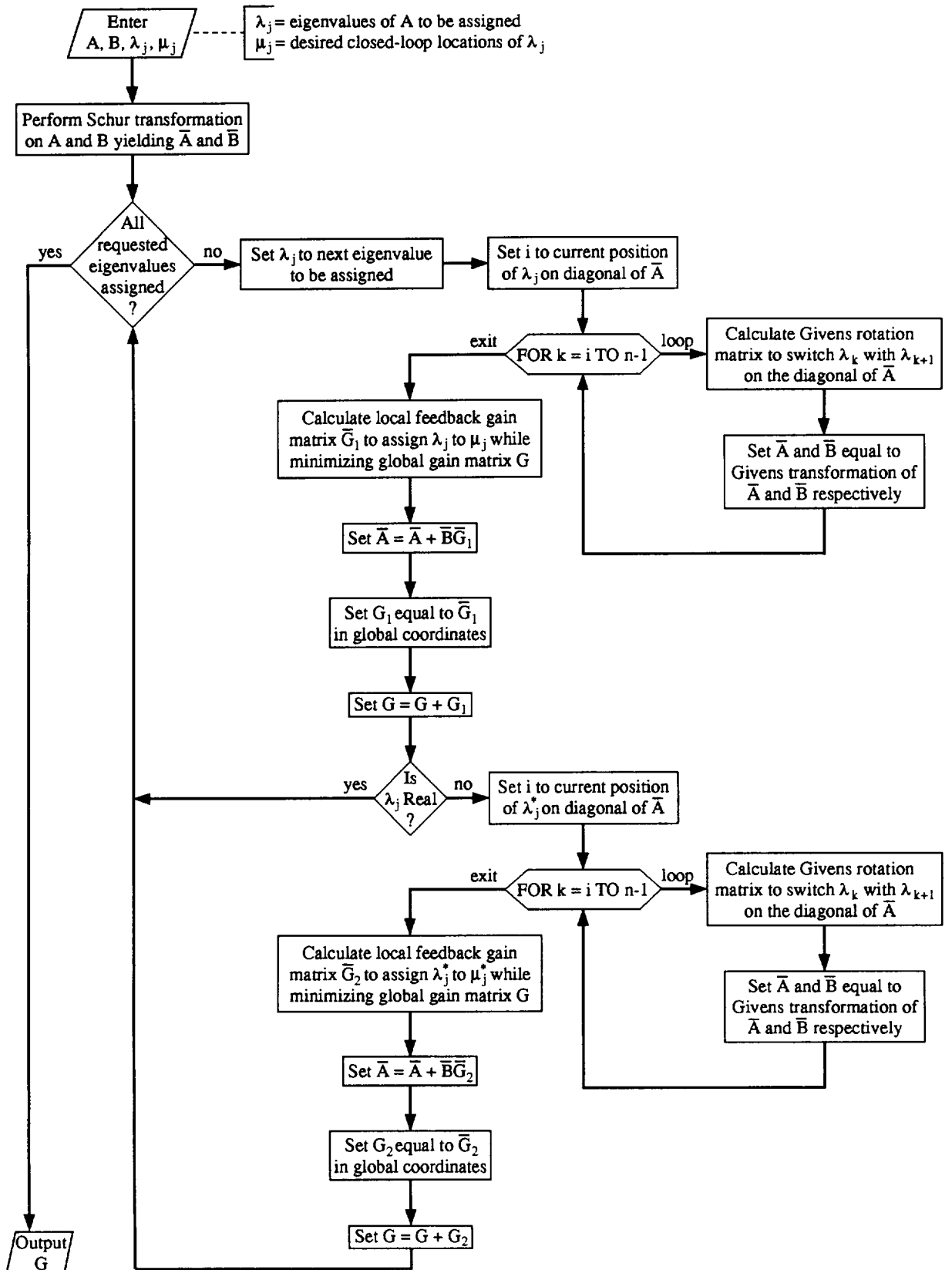


Figure 1. Flowchart of State Feedback EEA Algorithm

2.1.2 Sample Problem with Full-State Feedback

The eigenvalue assignment technique for full-state feedback can be clearly demonstrated with a sample problem. Let us consider the two degree of freedom, spring-mass-damper system illustrated in Figure 2.

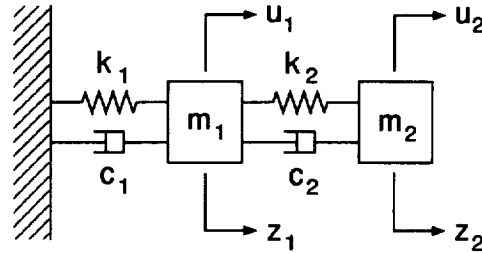


Figure 2. Spring-Mass-Damper System

The system has two force inputs, u_1 and u_2 , and two displacement outputs, $y_1=z_1$ and $y_2=z_2$. The two second order equations of motion that describe this system are as follows:

$$m_1 \ddot{z}_1 + (c_1 + c_2) \dot{z}_1 - c_2 \dot{z}_2 + (k_1 + k_2) z_1 - k_2 z_2 = u_1$$

$$m_2 \ddot{z}_2 - c_2 \dot{z}_1 + c_2 \dot{z}_2 - k_2 z_1 + k_2 z_2 = u_2$$

This system of equations can be converted to a first order state space form,

$$[\dot{x}] = A[x] + B[u]$$

$$[y] = C[x]$$

where,

$$A = \begin{bmatrix} 0 & 1 & 0 & 0 \\ -\frac{(k_1+k_2)}{m_1} & -\frac{(c_1+c_2)}{m_1} & \frac{k_2}{m_1} & \frac{c_2}{m_1} \\ 0 & 0 & 0 & 1 \\ \frac{k_2}{m_2} & \frac{c_2}{m_2} & -\frac{k_2}{m_2} & -\frac{c_2}{m_2} \end{bmatrix}$$

$$B = \begin{bmatrix} 0 & 0 \\ \frac{1}{m_1} & 0 \\ 0 & 0 \\ 0 & \frac{1}{m_2} \end{bmatrix}$$

$$C = \begin{bmatrix} 1 & 0 & 0 & 0 \\ 0 & 0 & 1 & 0 \end{bmatrix}$$

and the state variables are defined as,

$$\begin{bmatrix} x_1 \\ x_2 \\ x_3 \\ x_4 \end{bmatrix} = \begin{bmatrix} z_1 \\ \dot{z}_1 \\ z_2 \\ \dot{z}_2 \end{bmatrix}$$

Next we will assign numerical values to the physical constants. Let $m_1=1$ kg, $m_2=2$ kg, $k_1=1$ N/m, $k_2=1$ N/m, $c_1=6$ kg/s, and $c_2=5$ kg/s. Substituting these values into the state space equation, yields

$$A = \begin{bmatrix} 0.00 & 1.00 & 0.00 & 0.00 \\ -2.00 & -11.00 & 1.00 & 5.00 \\ 0.00 & 0.00 & 0.00 & 1.00 \\ 0.50 & 2.50 & -0.50 & -2.50 \end{bmatrix}$$

$$B = \begin{bmatrix} 0.00 & 0.00 \\ 1.00 & 0.00 \\ 0.00 & 0.00 \\ 0.00 & 0.50 \end{bmatrix}$$

$$C = \begin{bmatrix} 1.00 & 0.00 & 0.00 & 0.00 \\ 0.00 & 0.00 & 1.00 & 0.00 \end{bmatrix}$$

The eigenvalues of A are -0.18 , -0.23 , -1.00 , -12.09 . Using the full-state feedback technique described earlier, we will assign the first two eigenvalues to a desired location of -2.00 . In other words, we will determine a state feedback gain matrix so that the resulting closed-loop system will have the eigenvalues: -2.00 , -2.00 , -1.00 , -12.09 .

First the A matrix is transformed into Schur form, putting the eigenvalues along the main diagonal. \bar{A} will be used to denote A in transformed coordinates, and similarly for all other matrices in transformed coordinates.

$$\bar{A} = \begin{bmatrix} -12.09 & -2.14 & 2.26 & 2.74 \\ 0.00 & -0.18 & -0.06 & 1.01 \\ 0.00 & 0.00 & -0.23 & 0.72 \\ 0.00 & 0.00 & 0.00 & -1.00 \end{bmatrix}$$

The same transformation is applied to B , yielding

$$\bar{B} = \begin{bmatrix} 0.97 & -0.12 \\ 0.02 & -0.07 \\ -0.11 & -0.09 \\ 0.24 & 0.47 \end{bmatrix}$$

Now the first eigenvalue to be assigned must be isolated at the end of the main diagonal of \bar{A} . This is done through a series of Givens rotations. In this case we first wish to move -0.18 to the end of the diagonal of \bar{A} . The first Givens rotation switches the second and third elements on the main diagonal.

$$\bar{A} = \begin{bmatrix} -12.09 & -2.14 & 2.26 & 2.74 \\ 0.00 & -0.23 & -0.06 & 1.01 \\ 0.00 & 0.00 & -0.18 & 0.72 \\ 0.00 & 0.00 & 0.00 & -1.00 \end{bmatrix}$$

Another rotation switches the third and fourth elements, placing -0.18 at the end of the diagonal.

$$\bar{A} = \begin{bmatrix} -12.09 & -2.14 & 2.26 & 2.74 \\ 0.00 & -0.23 & -0.06 & 1.01 \\ 0.00 & 0.00 & -1.00 & 0.72 \\ 0.00 & 0.00 & 0.00 & -0.18 \end{bmatrix}$$

At the same time each of these Givens rotations was applied to \bar{B} , yielding

$$\bar{B} = \begin{bmatrix} 0.97 & -0.12 \\ -0.05 & -0.11 \\ 0.22 & 0.47 \\ 0.12 & 0.08 \end{bmatrix}$$

At this point a local gain matrix, \bar{G}_1 , is calculated to assign -0.18 to -2.00 without affecting the remaining eigenvalues. As described earlier, there is some flexibility in choosing a local gain matrix for this assignment. Therefore the gain matrix is also chosen to minimize the norm of the global gain matrix, which is the sum of all the previous local gain matrices. At this point there are no previous local gain matrices, so \bar{G}_1 is calculated to be the local gain matrix with the minimum norm. The current \bar{A} matrix is then updated by $\bar{A} \equiv \bar{A} + \bar{B}\bar{G}_1$, yielding

$$\bar{A} = \begin{bmatrix} -12.09 & -2.14 & 2.26 & 2.74 \\ 0.00 & -0.23 & -0.06 & 1.01 \\ 0.00 & 0.00 & -1.00 & 0.72 \\ 0.00 & 0.00 & 0.00 & -2.00 \end{bmatrix}$$

\bar{G}_1 is then transformed back to the original coordinate system, and this gain matrix, denoted G_1 , will be used in the calculation of the global gain matrix. G_1 for the first

eigenvalue assignment is

$$G_1 = \begin{bmatrix} -10.07 & -1.31 & 2.74 & -1.64 \\ -6.30 & -0.82 & 1.72 & -1.03 \end{bmatrix}$$

This is also equal to the current global gain matrix, G .

Now a new series of Givens rotations are used to move -0.23 to the end of the main diagonal of \bar{A} . The result of which is

$$\bar{A} = \begin{bmatrix} -12.09 & -2.14 & 2.26 & 2.74 \\ 0.00 & -1.00 & -0.06 & 1.01 \\ 0.00 & 0.00 & -2.00 & 0.72 \\ 0.00 & 0.00 & 0.00 & -0.23 \end{bmatrix}$$

The Givens rotations are also applied to \bar{B} . An optimum local gain matrix is calculated to assign -0.23 to -2.00 . \bar{A} is updated with the new \tilde{G}_1

$$\bar{A} = \begin{bmatrix} -12.09 & -2.14 & 2.26 & 2.74 \\ 0.00 & -1.00 & -0.06 & 1.01 \\ 0.00 & 0.00 & -2.00 & 0.72 \\ 0.00 & 0.00 & 0.00 & -2.00 \end{bmatrix}$$

The new \tilde{G}_1 is transformed back to the original coordinate system, yielding

$$G_1 = \begin{bmatrix} -2.21 & -0.12 & 1.40 & 0.36 \\ 20.34 & 1.11 & -12.91 & -3.29 \end{bmatrix}$$

This is added to the previous G_1 to produce the final global gain matrix

$$G = \begin{bmatrix} -12.28 & -1.43 & 4.14 & -1.28 \\ 14.04 & 0.29 & -11.19 & -4.32 \end{bmatrix}$$

With all the desired eigenvalues placed, this G is the final feedback gain matrix. The closed-loop state matrix formed with this G is $A_{CL} = A + BG$ and

$$A_{CL} = \begin{bmatrix} 0.00 & 1.00 & 0.00 & 0.00 \\ -14.28 & -12.43 & 5.14 & 3.72 \\ 0.00 & 0.00 & 0.00 & 1.00 \\ 7.52 & 2.65 & -6.10 & -4.66 \end{bmatrix}$$

The eigenvalues of A_{CL} are $-1.00, -2.00, -2.00, -12.09$.

This numerical example illustrates the sequential eigenvalue assignment employed by EEA using full-state feedback. Desired eigenvalues are assigned without shifting the

remaining ones. One can see how this technique is especially efficient when the number of assigned eigenvalues is smaller than the order of the system. In the next section the EEA algorithm using output feedback will be discussed.

2.2. Output Feedback

Since full-state feedback may not be available for implementation in many real applications, an EEA procedure using output feedback was also developed by Maghami and Juang in [8]. In this section the theory behind output feedback eigenvalue assignment will be discussed, as described by Maghami and Juang. Also a new enhancement to this algorithm is described, which attempts to overcome the major shortcoming that the stability of the resulting closed-loop system is not guaranteed for all output feedback eigenvalue assignment techniques, including Maghami and Juang's.

2.2.1 Theory

Maghami and Juang point out that for (almost all) fully controllable and observable systems, with m inputs and p outputs, $\min(m + p - 1, n)$ eigenvalues of the system may be arbitrarily assigned with real gains. The closed-loop dynamics of the system with output feedback is given as

$$\dot{\mathbf{x}}(t) = [A + BGC]\mathbf{x}(t) \quad (2.16)$$

where G is an $m \times p$ output feedback gain matrix, and A , B , C , and $\mathbf{x}(t)$ have been previously defined.

Maghami and Juang's output feedback algorithm works in two steps to assign the maximum allowable number of eigenvalues. First, \bar{m} pairs of eigenvalues may be assigned, where $2\bar{m} \leq m - 1$, via any of the output feedback methods outlined in the literature [3], [4], [22]. For this discussion we shall be considering the case where

all the system eigenvalues are complex. These initially assigned eigenvalues are kept unchanged during the next step, where the remaining p eigenvalues are placed to the desired values. The output feedback gain matrix for the entire assignment is then the sum of the gain matrices obtained from each step. One of the major shortcomings of output feedback eigenvalue assignment techniques, including this one, is that the stability of the resulting closed-loop system is not guaranteed (an attempt to resolve this problem will be discussed in Section 2.2.2).

If we assume that the A matrix in Eq. (2.16) is the closed-loop state matrix after the initial assignment of eigenvalues, then we can begin with a detailed description of the second part of the output feedback algorithm. As with the state feedback algorithm, a Schur transformation is applied to the system placing the eigenvalues along the main diagonal of A . Next, the previously assigned eigenvalues, or the open-loop eigenvalues selected to be kept unchanged, are moved to the end of the diagonal via Givens transformations. The resulting closed-loop system becomes

$$\dot{\bar{x}}(t) = [\bar{A} + \bar{B}G\bar{C}]\bar{x}(t) \quad (2.17)$$

where $\bar{x}(t) = Lx(t)$, $\bar{A} = L^H A L$, $\bar{B} = L^H B$, $\bar{C} = C L$, and L is the cumulative transformation matrix defined as $L = V R_1 \cdots R_s$.

Let $\bar{B}_{\bar{m}}$ denote the last $2\bar{m}$ rows of \bar{B} . Then, it is obvious that if the columns of G are chosen to lie in the right null space of $\bar{B}_{\bar{m}}$, the feedback return matrix $\bar{B}G\bar{C}$ will not affect the \bar{m} pairs of eigenvalues at the end of the diagonal of \bar{A} . Defining Ψ as an orthonormal basis spanning the right null space of matrix $\bar{B}_{\bar{m}}$, i.e.,

$$\bar{B}_{\bar{m}}\Psi = 0 \quad (2.18)$$

the gain matrix G can be expanded in terms of Ψ

$$G = \Psi q \quad (2.19)$$

in which q is an $r \times p$ coefficient matrix, and r denotes the dimension of the null basis. The eigenvalue assignment problem is now reduced to finding a set of coefficients q that assigns the remaining p eigenvalues of the following subsystem

$$\dot{\bar{x}}_r(t) = [\bar{A}_r + \bar{B}_r \Psi q \bar{C}_r] \bar{x}_r(t) \quad (2.20)$$

where \bar{A}_r , \bar{B}_r , and \bar{C}_r are submatrices composed of the first $(n - 2\bar{m})$ rows and columns of \bar{A} , the first $(n - 2\bar{m})$ rows of \bar{B} , and the first $(n - 2\bar{m})$ columns of \bar{C} , respectively. Here \bar{x}_r denotes the first $(n - 2\bar{m})$ elements of \bar{x} . Since all the variables in Eq. (2.20) are complex, the task of assigning the desired eigenvalues may be quite cumbersome. However, due to the unique nature of the Schur vectors a more amenable and computationally efficient companion system may be considered instead as follows:

$$\dot{z}(t) = [A_c + B\Psi qC]z(t) \quad (2.21)$$

where A_c is an $n \times n$ matrix defined as

$$A_c = L \begin{bmatrix} \bar{A}_r & 0 \\ 0 & 0 \end{bmatrix} L^H$$

and $z(t)$ is a companion state vector. The eigenvalues of A_c are the same as eigenvalues of \bar{A}_r except for \bar{m} pairs of additional zero eigenvalues, which will similarly not be affected by the feedback return of $B\Psi qC$. All the variables in Eq. (2.21) are real except Ψ and q . Since only real-valued gain matrices are meaningful, the gain matrix in Eq. (2.21) is replaced by the real part, such that

$$\dot{z}(t) = [A_c + B(\Psi_R q_R - \Psi_I q_I)C]z(t) \quad (2.22)$$

Now every variable in Eq. (2.22) is real. The eigenvalue problem for Eq. (2.22) is given by

$$[A_c + B(\Psi_R q_R - \Psi_I q_I)C]\eta_k = \eta_k \bar{\mu}_k \quad (2.23)$$

where η_k and $\bar{\mu}_k$, respectively, denote the k th eigenvector and desired eigenvalue. Expanding Eq. (2.23) in terms of real and imaginary parts of η_k and $\bar{\mu}_k$ and rearranging the results in matrix form yields

$$\Gamma_k \begin{bmatrix} \eta_{kR} \\ \eta_{kI} \\ q_R C \eta_{kR} \\ q_I C \eta_{kR} \\ q_R C \eta_{kI} \\ q_I C \eta_{kI} \end{bmatrix} \equiv \Gamma_k \phi_k = 0 \quad (2.24)$$

where

$$\Gamma_k = \begin{bmatrix} A_c - \mu_{kR} I_n & \mu_{kI} I_n & B \hat{\Psi} & 0 \\ -\mu_{kI} I_n & A_c - \mu_{kR} I_n & 0 & B \hat{\Psi} \end{bmatrix}$$

and $\hat{\Psi} = [\Psi_R \quad -\Psi_I]$. Equation (2.24) is satisfied for each pair of complex conjugate eigenvalues. Let v_k denote an orthonormal basis for the solution of Eq. (2.24) that spans the null space of Γ_k . If s pairs of eigenvalues are to be assigned, then the solution of the homogeneous equation of Eq. (2.24) may be written for the k th pair ($k = 1, \dots, s$) as

$$\Gamma_k \phi_k \equiv \Gamma_k \begin{bmatrix} \phi_{kR} \\ \phi_{kI} \\ \phi_{kRR} \\ \phi_{kRI} \\ \phi_{kIR} \\ \phi_{kII} \end{bmatrix} = \Gamma_k \begin{bmatrix} v_{kR} \\ v_{kI} \\ v_{kRR} \\ v_{kRI} \\ v_{kIR} \\ v_{kII} \end{bmatrix} c_k = 0 \quad (2.25)$$

where the null basis v_k has been partitioned into six components according to Eq. (2.24), and c_k are the appropriate coefficients for the basis v_k . Comparison of Eq. (2.24) and (2.25) yields that the matrices q_R and q_I must satisfy

$$q_R C [\phi_{kR}, \phi_{kI}] = [\phi_{kRR}, \phi_{kIR}]; \quad k = 1, \dots, s \quad (2.26)$$

$$q_I C [\phi_{kR}, \phi_{kI}] = [\phi_{kRI}, \phi_{kII}]; \quad k = 1, \dots, s \quad (2.27)$$

It is observed from Eq. (2.25) that any freedom provided by the multi-inputs and multi-outputs is imbedded in the coefficients c_k . This freedom can be exploited to achieve better closed-loop criterion such as minimizing a weighted norm of the gain

matrix or, as will be discussed in the next section, achieving guaranteed closed-loop stability. However, as long as the coefficients c_k are chosen to generate a set of linearly independent eigenvectors, a solution for the gain matrix can be obtained.

Equations (2.26) and (2.27) can be written in a general matrix form

$$q_R \Phi = \hat{\Phi} \quad (2.28)$$

$$q_I \Phi = \bar{\Phi} \quad (2.29)$$

in which

$$\Phi = C[\phi_{1R}, \phi_{1I}, \dots, \phi_{sR}, \phi_{sI}]$$

$$\hat{\Phi} = [\phi_{1RR}, \phi_{1IR}, \dots, \phi_{sRR}, \phi_{sIR}]$$

$$\bar{\Phi} = [\phi_{1RI}, \phi_{1II}, \dots, \phi_{sRI}, \phi_{sII}]$$

The solution for q_R and q_I is then given as

$$q_R = \hat{\Phi}[\Phi]^\dagger \quad (2.30)$$

$$q_I = \bar{\Phi}[\Phi]^\dagger \quad (2.31)$$

where $[\]^\dagger$ is the pseudoinverse. Note that the solutions given in Eq. (2.30) and (2.31) are unique or minimum norm depending on the number of pairs assigned. With q_R and q_I determined, the output feedback gain matrix G is computed as

$$G = \Psi_R q_R - \Psi_I q_I \quad (2.32)$$

It can be shown that the columns of the gain matrix G satisfy the orthogonality condition of Eq. (2.18) provided that \bar{m} pairs of eigenvalues assigned previously are either real or complex conjugates. The procedure discussed here can assign up to $\min(m + p - 1, n)$ eigenvalues with output feedback.

2.2.2 Optimized Output Feedback

The output feedback EEA algorithm developed by Maghami and Juang [8] is a computationally reliable control design tool. However, when it is applied to real systems, such as the control of large space structures, the drawback of unguaranteed stability can make it unviable in some cases. This is also true for most output feedback eigenvalue assignment algorithms. The EEA technique can only enhance the possibility of achieving a stable solution by imposing constraints on some of the most sensitive open-loop eigenvalues. Nevertheless, the method does quantify the freedom in the calculation of the final feedback gain matrix. It is proposed to exploit this freedom through optimization to produce a stable closed-loop system.

The previous section detailed how the eigenvector coefficients c_k in Eq. (2.25) contained the freedom to provide different feedback gain solutions. The solution to the eigenvalue assignment problem is nonunique, and arbitrary choices of c_k produce different gain matrices, each of which will assign the $\min(m + p - 1, n)$ eigenvalues of the system. However for the case where $m + p - 1 < n$, each choice of c_k will effect the closed-loop values of the remaining $n - (m + p - 1)$ eigenvalues. It is these remaining eigenvalues that can cause the nominal closed-loop system to be unstable. Therefore, one would like to find the values of c_k that would produce a stable closed-loop system and, since the flexibility exists, minimize the norm of the gain matrix. This can be accomplished by delegating the choice of c_k to a constrained nonlinear optimization that minimizes the norm of the resulting gain matrix subject to the constraints that the real parts of all the remaining $n - (m + p - 1)$ eigenvalues are less than zero or less than some specified limit.

The constrained nonlinear optimization problem can be posed mathematically as

$$\begin{aligned} \min_{c_k} : f(c_k) &= |G|_F \\ \text{constraint : } \text{real}(\lambda_{cl}) &< 0 \end{aligned} \tag{2.33}$$

where $|G|_F$ denotes the Frobenius norm of the feedback gain matrix and λ_{cl} denotes the eigenvalues of the closed-loop system $(A + BGC)$. Figure 3 shows how this proposed optimization is incorporated into the output feedback algorithm.

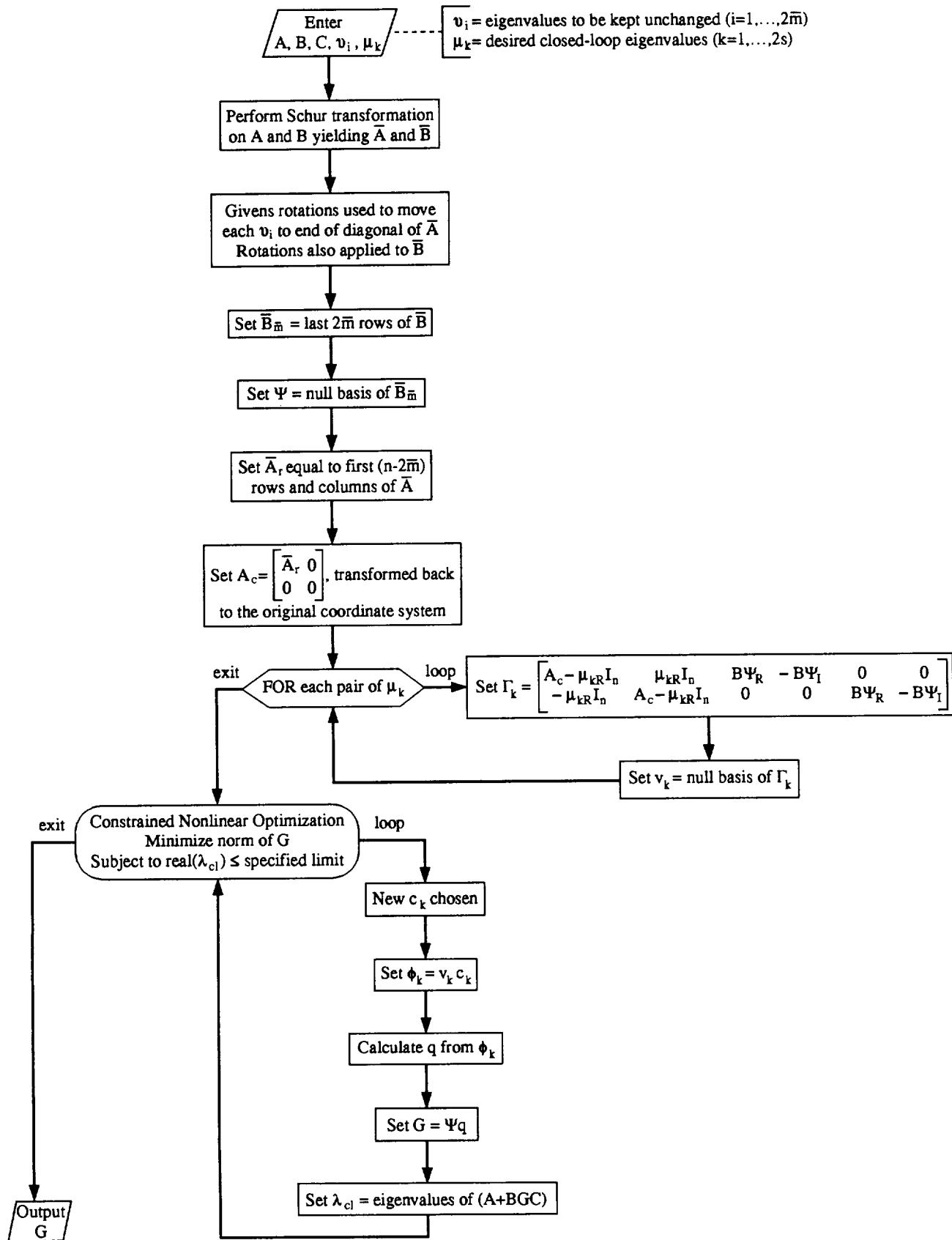


Figure 3. Flowchart of Optimized Output Feedback EEA Algorithm

3. IMPLEMENTATION OF STATE FEEDBACK EFFICIENT EIGENVALUE ASSIGNMENT CONTROLLER ON PHASE 2 CEM

A series of controllers based on the state feedback EEA algorithm were designed and tested on the Phase 2 configuration of the CSI Evolutionary Model (CEM). The Phase 2 CEM is one in a sequence of laboratory models, developed at NASA Langley Research Center, to explore improved ways to model, control, and design space structures [30]. The purpose of these experiments was to experimentally verify controller design software based on the EEA methods described in [8] as well as to verify the methods themselves.

3.1. Phase 2 CEM Description

The Phase 2 CEM, shown in Figure 4, consists of an aluminum truss structure 620 inches long and 110 inches wide, constructed from 10 inch cubical bays. The structure has a 62 bay long main truss, four 10 bay horizontal suspension trusses, an 11 bay vertical laser tower, and a four bay vertical reflector tower. There are three two axis gimbals mounted on the main truss, a 17 inch diameter reflector mounted on top of the tower at the aft end of the structure, and a laser source mounted on top of the other tower. The structure is suspended from the ceiling (about 840 inches above the main truss) by four cables as shown. Each of these cables are in turn connected to pneumatic-magnetic suspension devices which are used to simulate a near zero gravity condition. Eight proportional bi-directional air thrusters, with a maximum output force of 4.4 lbs each, provide the input actuation, while collocated servo accelerometers provide output measurements. Because the controllers designed for the structure used velocity feedback, the acceleration measurements were passed through an integrator to produce velocity measurements. For the following series of tests to be described, the laser source and reflector, used to provide information on the global line-of-sight pointing accuracy, and

the three gimbals, used to simulate the interaction of science instruments and the control systems with the spacecraft, were not used.

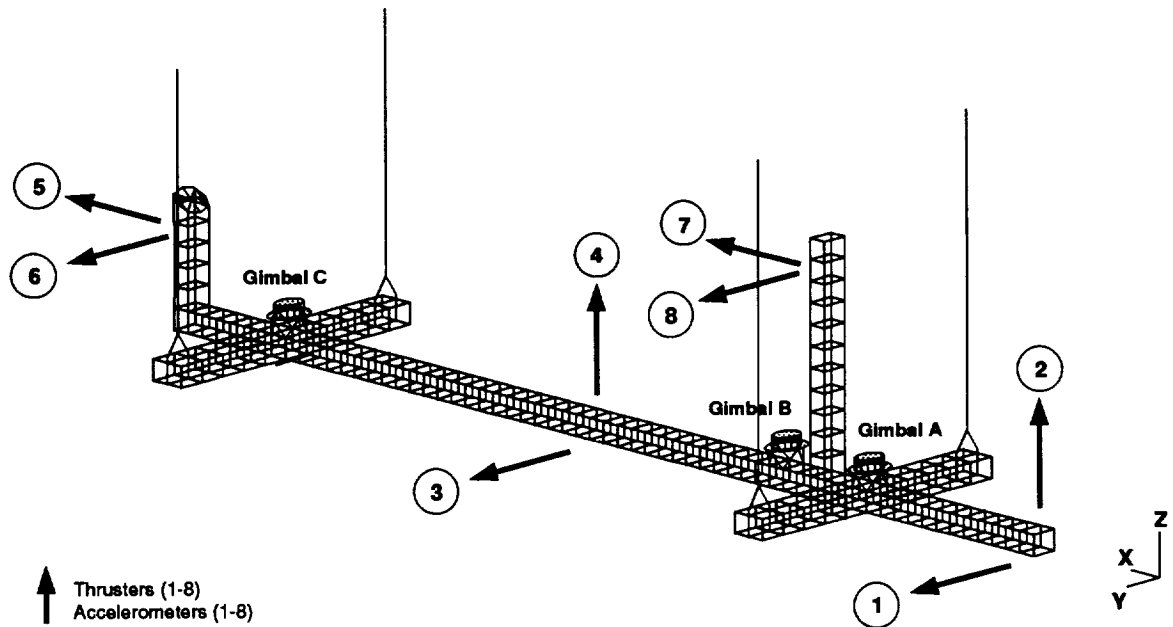


Figure 4. CSI Evolutionary Model - Phase 2

3.2. Modeling of Phase 2 CEM

It was necessary to generate a mathematical model of the Phase 2 CEM for design and simulation. The equations of motion for the structure can be written in a second-order form as

$$M\ddot{z} + D\dot{z} + Kz = Fu \quad (3.1)$$

where M , D , and K are the mass, damping, and stiffness matrices, respectively; z is the displacement vector; u denotes the control input; and F is the input influence matrix characterizing the locations and types of input.

Now let us assume that there is no damping in the system. This leaves us with

$$M\ddot{z} + Kz = Fu$$

In order to solve the homogeneous equation

$$M\ddot{\mathbf{z}} + K\mathbf{z} = 0 \quad (3.2)$$

a solution is assumed to be of the form

$$\{\mathbf{z}(t)\} = \{\mathbf{Z}\} e^{i\omega t}$$

Substituting this assumed solution into Eq (3.2) yields

$$(K - \omega^2 M)\{\mathbf{Z}\} = \{0\} \quad (3.3)$$

or for a particular mode

$$(K - \omega_j^2 M)\Phi_j = \{0\} \quad (3.4)$$

where ω_j and Φ_j represent the natural frequency and the structural normal mode shape, respectively, for mode j . From Eq. (3.4) we can obtain the following properties,

$$\Phi^T M \Phi = I \quad (3.5)$$

$$\Phi^T K \Phi = \begin{bmatrix} -\omega_1^2 & & & 0 \\ & -\omega_2^2 & & \\ & & \dots & \\ 0 & & & -\omega_q^2 \end{bmatrix} \quad (3.6)$$

and with the assumption of modal damping, we have

$$\Phi^T D \Phi = \begin{bmatrix} -2\zeta_1\omega_1 & & & 0 \\ & -2\zeta_2\omega_2 & & \\ & & \dots & \\ 0 & & & -2\zeta_q\omega_q \end{bmatrix} \quad (3.7)$$

where ζ_j represents the damping ratio of mode j , and q represents the number of modes used to construct the model.

Now we wish to express Eq. (3.1) in a first-order form by defining the vector \mathbf{x} as

$$\mathbf{x} = \begin{bmatrix} \mathbf{z} \\ \dot{\mathbf{z}} \end{bmatrix} \quad (3.8)$$

to reduce the number of computations required, the resulting model was constructed with only 20 modes. Because damping for a complex structure is difficult to model, a modal damping ratio of 0.1% was assumed for all modes. The Phase 2 CEM state space model was constructed using Eqs. (3.13), (3.14), and the modal parameters described above. This 20 mode model was used to design the following controllers.

3.3. Controller Design and Phase 2 CEM Implementation

The EEA algorithms were programmed in MATLAB M-files. Both full-state feedback and output feedback versions were programmed; however, during the time allotted for testing on Phase 2, only an output feedback version without optimization was completed. This output feedback version did not provide stabilizing controllers for the Phase 2 CEM. Therefore, only controllers designed using state feedback were implemented on the structure.

The state feedback eigenvalue assignment program requires the user to supply the state and input matrices and to specify which open-loop eigenvalues are to be assigned and the desired locations of these eigenvalues. The program then computes the full-state feedback gain matrix required to place only the specified open-loop eigenvalues to the desired locations without effecting the remaining eigenvalues.

Since full-state feedback is not available for the Phase 2 structure, a Kalman filter was used in series with the controller to provide estimates of the full state from the velocity signals integrated from all eight accelerometers. The Kalman filter was designed using the linear quadratic estimator function supplied in the MATLAB Control System Toolbox [31]. The weighting matrices were chosen to produce an estimator with poles at least twice as fast as the closed-loop system poles. In general, the designed estimator had a majority of the poles about six times as fast as the closed-loop system poles.

Using the EEA program, a series of controllers were designed for Phase 2 CEM. The goal of each controller was to increase the damping of the first two flexible body modes of vibration in the Phase 2 structure without effecting the open-loop frequencies. As shown in Table 1 the first two flexible body modes of Phase 2 are the seventh and eighth modes of vibration. Having decided that the controller would place the two pairs of eigenvalues associated with modes seven and eight, the desired closed-loop eigenvalues reflecting a new level of damping had to be calculated. This was done as follows:

A complex conjugate pair of eigenvalues can be represented as

$$\lambda = -\zeta\omega_n \pm j\omega_n\sqrt{1-\zeta^2}$$

where ζ is the damping ratio, and ω_n is the undamped natural frequency. The objective is to produce a new eigenvalue pair with the same undamped natural frequency and a new damping ratio, which we will call $\bar{\zeta}$. The new eigenvalue pair would then have the form

$$\mu = -\bar{\zeta}\omega_n \pm j\omega_n\sqrt{1-\bar{\zeta}^2}$$

where ω_n is either calculated from the real and imaginary parts of λ or taken directly from the finite element model data. Thus the complex conjugate pairs of μ are the desired closed-loop eigenvalues.

Table 1. Phase 2 CEM – Measured Open-Loop Modal Information

	Mode	Frequency (Hz)	Damping (%)	Description
Rigid Body Modes	1	0.132	5.503	Yaw
	2	0.135	4.576	X Pendulum
	3	0.136	3.658	Y Pendulum
	4	0.180	5.807	Bounce (node near laser tower)
	5	0.192	5.885	Bounce (node near reflector tower)
	6	0.344	2.420	Roll
Flexible Body Modes	7	1.767	0.238	1st Torsion
	8	2.432	0.178	1st X-Z Bending
	9	3.049	0.291	1st X-Y Bending
	10	5.689	0.183	2nd X-Z Bending
	11	6.137	0.175	Reflector Appendage Rocking
	12	6.451	0.575	Reflector Appendage Rocking
	13	6.577	0.202	Reflector Appendage Rocking
	14	6.734	0.366	Reflector Appendage Rocking
	15	7.218	0.195	Cable
	16	7.777	0.236	Laser Tower X-Z Bending
	17	8.719	0.250	2nd X-Y Bending
	18	9.146	0.177	2nd X-Z Bending
	19	10.212	0.206	Laser Tower Y-Z Bending
	20	13.087	0.057	3rd X-Y Bending

The EEA program is ideally suited to produce controllers to increase the damping on certain modes of the Phase 2 structure as this controller design makes use of the efficiency of the algorithm because the number of eigenvalues to be assigned is much less than the order of the system. The assignment algorithm also assures that the open-loop modal parameters of the other modes remain unchanged.

3.4. Test Procedure and Results

After the closed-loop systems were simulated and verified in MATLAB, the EEA controllers were tested on the Phase 2 structure. Each controller was designed to produce a different level of modal damping. Table 2 lists these tests. The procedure for each 40 second test consisted of 10 seconds of open-loop sinusoidal excitation of the structure using the air thrusters, followed by one second of free decay, then during the remaining 29 seconds the controller command loops were closed. In the case of the open-loop tests (Tests 1 and 12), the final 30 seconds were all free decay. Through inspection of the input matrix, it was determined which thruster should be used to excite a given mode to provide the optimum excitation in that mode. This was done by identifying the largest positive number in the row of the input matrix that pertains to the mode to be excited. The number of the column that contains this number is the number of the thruster that should be used to provide the most efficient excitation. In tests 1 through 11, sinusoidal command inputs were given to thrusters 8 and 4 at frequencies of 1.7074 Hz and 2.3782 Hz respectively. This predominantly excited only the first torsional mode and the first X-Z bending mode at the natural frequencies. In tests 12 and 13, in addition to thrusters 8 and 4, thrusters 1 and 5 were fired at frequencies of 0.1302 Hz and 0.1321 Hz respectively to also excite the first two rigid body modes. Test 13 was done to evaluate that the controller does not become unstable when modes other than those being controlled are also excited. In all the tests the amplitude of the sinusoidal thruster inputs were 2.0 volts or 0.81 lbf of thrust.

In order to check the performance of each controller, the desired damping for a given mode must be compared with the closed-loop damping obtained for that mode. An eigensystem realization algorithm using data correlation (ERA/DC) [32] was employed on the time response data from all eight accelerometers for each test to determine the modal parameters for each closed-loop system. The results of this analysis are also shown

in Table 2. The ERA/DC analysis was able to identify the modal parameters of the modes with substantial excitation. However, the accuracy of the ERA/DC analysis for modes with less excitation was poor, particularly in reference to the modal damping. This loss of accuracy prevents an evaluation of the non-controlled modes to determine whether they were affected by the state feedback controller. Nevertheless, since modes seven and eight were substantially excited, there is a high level of confidence in the modal parameters obtained for these modes by ERA/DC.

Table 2. Phase 2 CEM – Performance of EEA Controller

Test	Description	Desired Damping of Mode (%)		Measured Damping of Mode (%) *		Measured Frequency of Mode (Hz) *	
		7	8	7	8	7	8
1	Excitation of modes 7,8 Open-loop response	-	-	0.238	0.178	1.767	2.432
2	Excitation of modes 7,8 Eigenvalue placement of modes 7,8	1.000	1.000	1.258	1.022	1.778	2.449
3		1.500	1.500	1.813	1.506	1.782	2.458
4		2.000	2.000	2.369	1.986	1.789	2.464
5		3.000	3.000	3.356	2.941	1.796	2.477
6		4.000	4.000	4.405	3.685	1.806	2.491
7		6.000	6.000	5.911	5.295	1.827	2.521
8		8.000	8.000	7.358	6.585	1.849	2.551
9		10.000	10.000	8.628	7.651	1.867	2.582
10		12.000	12.000	10.873	7.865	1.912	2.626
11		15.000	15.000	11.703	8.280	1.942	2.676
12	Excitation of modes 1,2,7,8 Open-loop response	-	-	0.241	0.203	1.778	2.433
13	Excitation of modes 1,2,7,8 Eigenvalue placement of modes 7,8	10.000	10.000	8.933	7.975	1.902	2.593

* Measured using ERA/DC analysis of time response data

During each test the data from all eight accelerometers and thrusters was recorded. Figures 5-10 show the closed-loop time responses compared to the open-loop time responses for selected tests. For clarity and brevity only the data for the accelerometer/thruster pairs 8 and 4 are shown in Figures 5-8. These time response graphs best reflect the movement of the structure. For Test 13, shown in Figures 9 and 10 in which four modes are excited, the data for the accelerometer/thruster pairs 1, 5, 8 and 4 are shown.

One can see in all the plots of accelerometer data the shorter settling time of the closed-loop stem compared to the open-loop system. Figures 7 and 8, which show data from Tests 9 and 11, respectively, best illustrate the reduced settling time. Both of these closed-loop tests produce a settling time under five seconds, compared to over 30 seconds for the open-loop system.

The plots of thruster data shown in Figures 5 to 10 reveal the relatively low command power that was necessary to change the damping of the structure. This was due to the small norm of the feedback gain matrices calculated by the EEA algorithm. The thrusters can supply a maximum force of 4.4 lbs, which is achieved with a thruster command signal of 10.9 volts. In all the tests conducted the thrusters were never commanded to fire over 1.62 lbs of force or 4.0 volts.

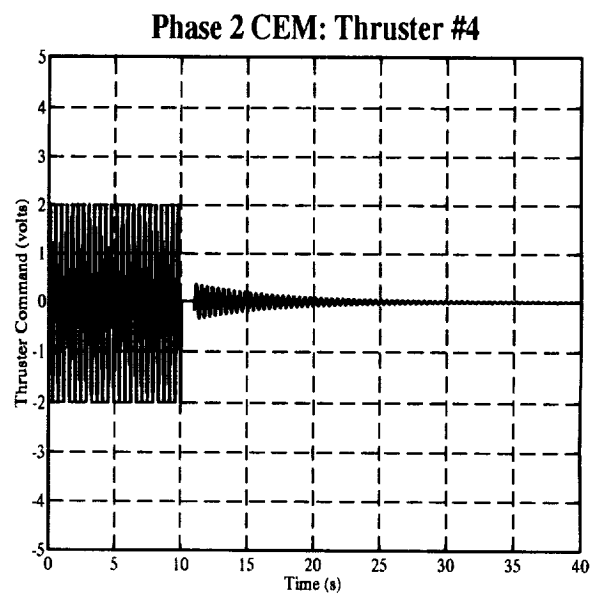
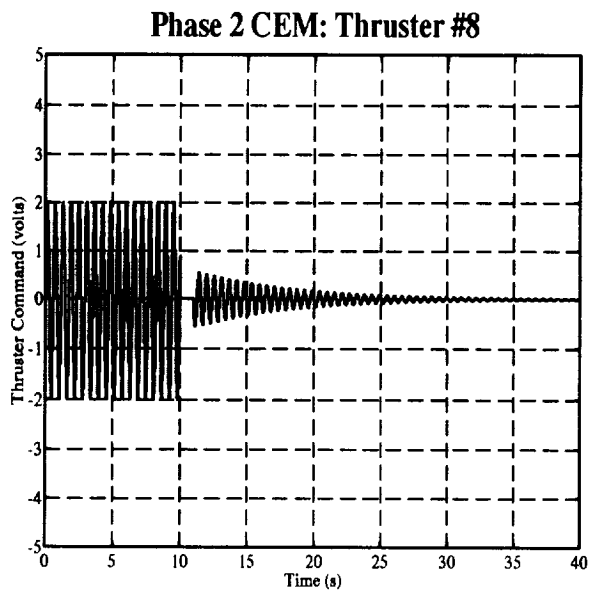
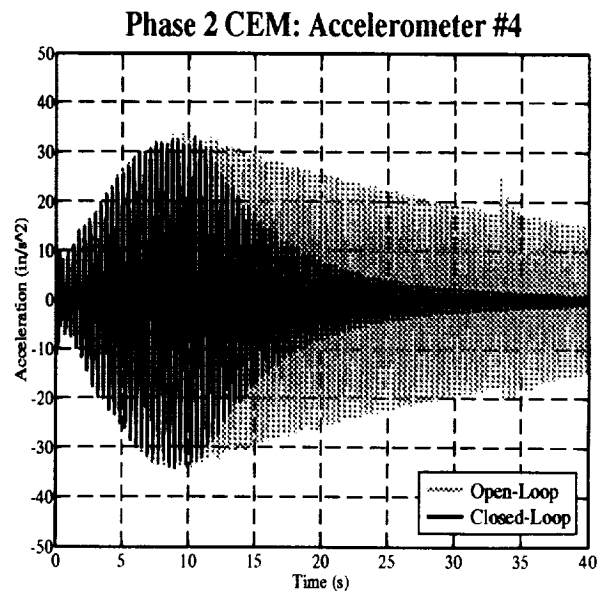
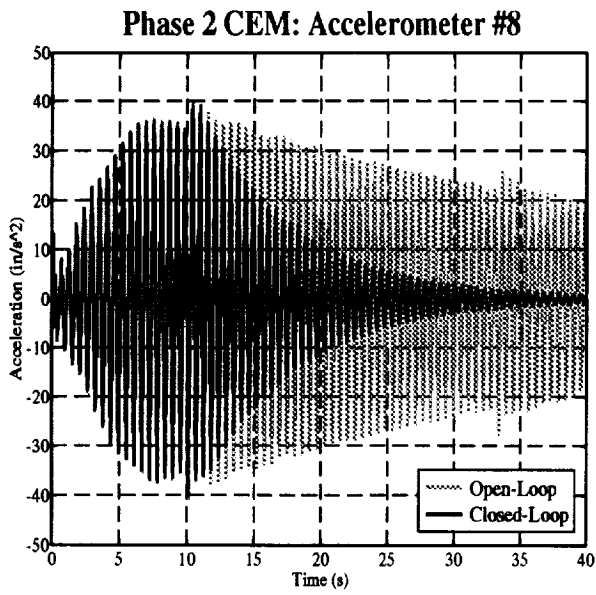


Figure 5. State Feedback Test 2: Closed-Loop versus Open-Loop Time Response

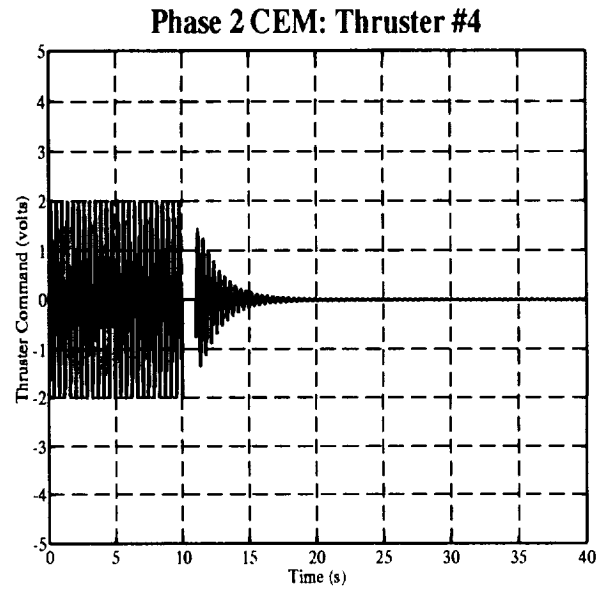
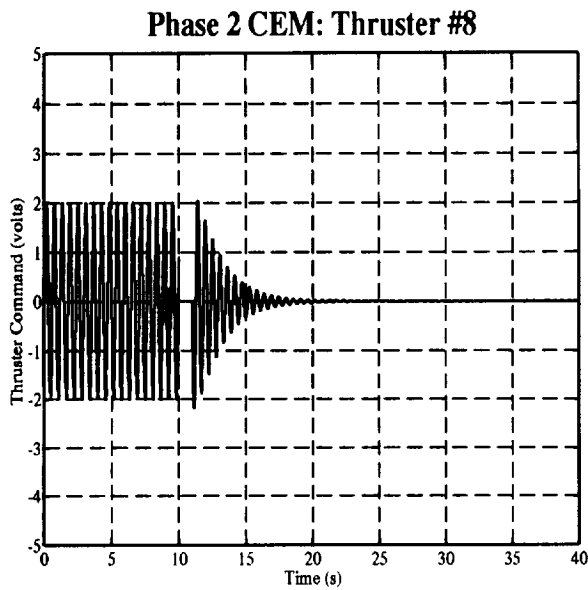
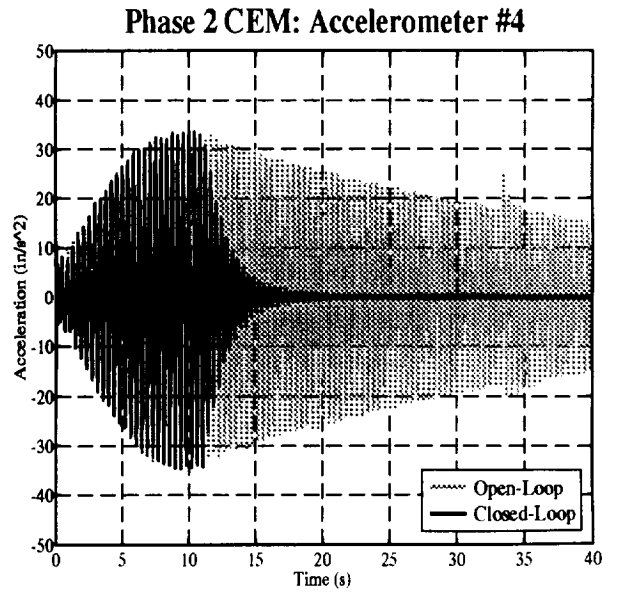
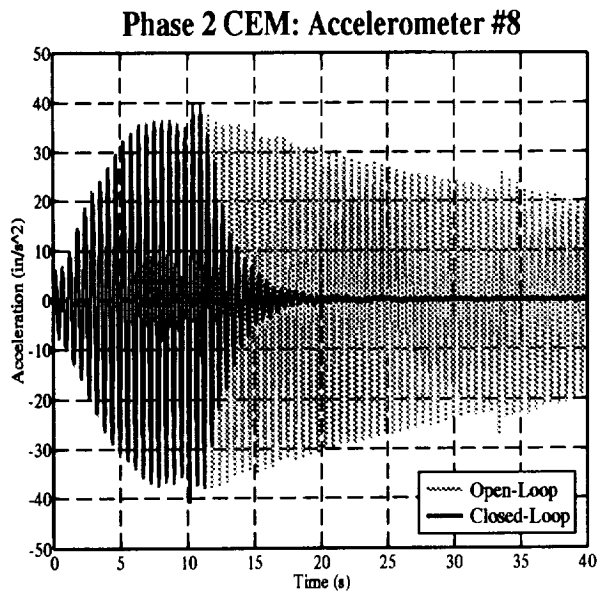


Figure 6. State Feedback Test 6: Closed-Loop versus Open-Loop Time Response

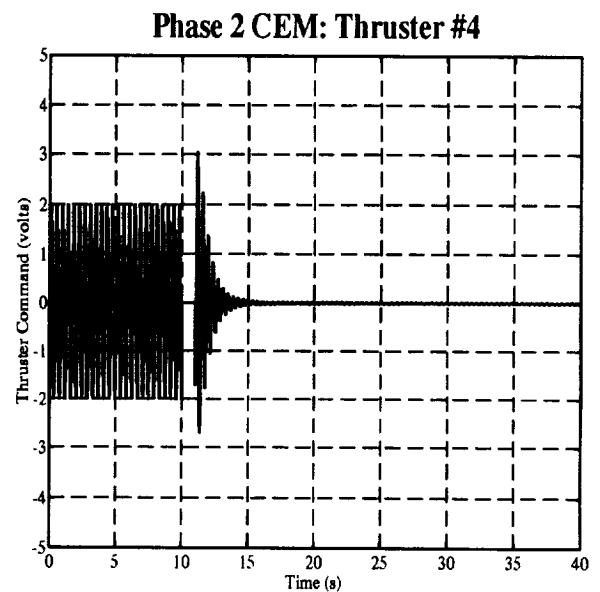
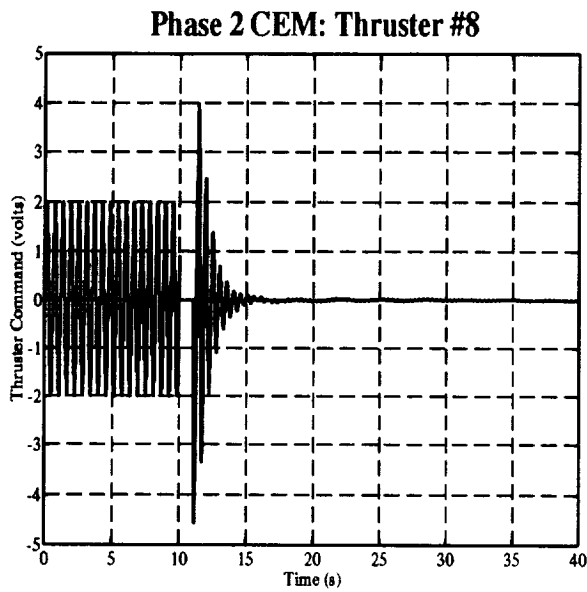
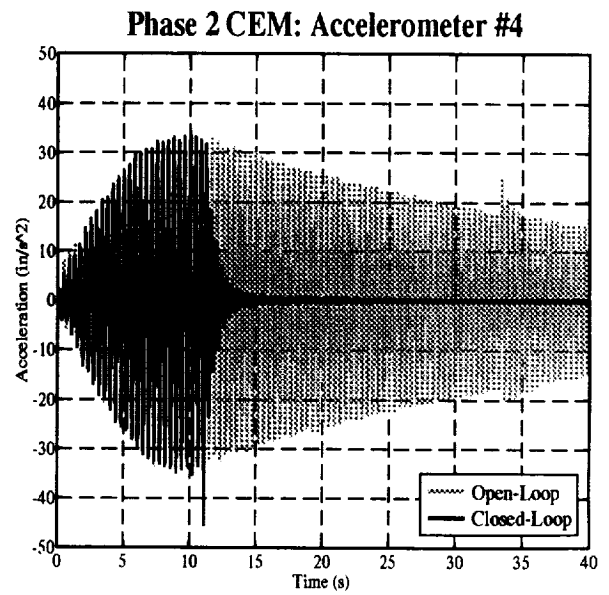
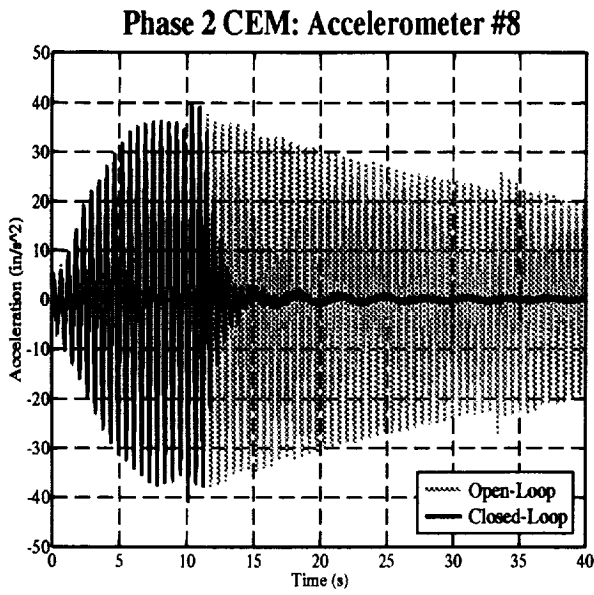


Figure 7. State Feedback Test 9: Closed-Loop versus Open-Loop Time Response

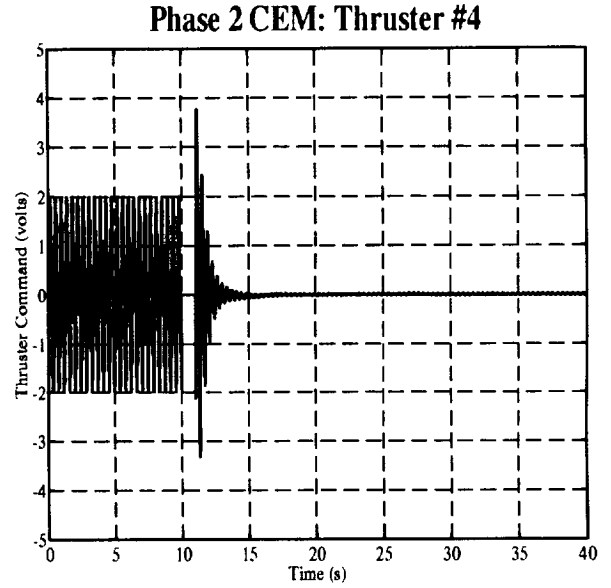
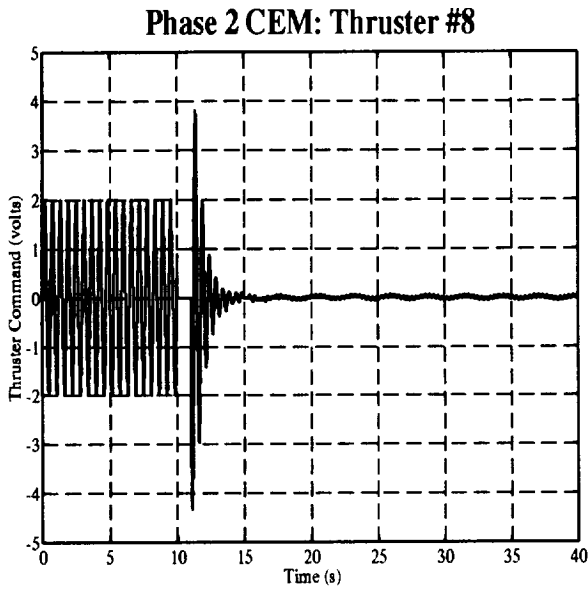
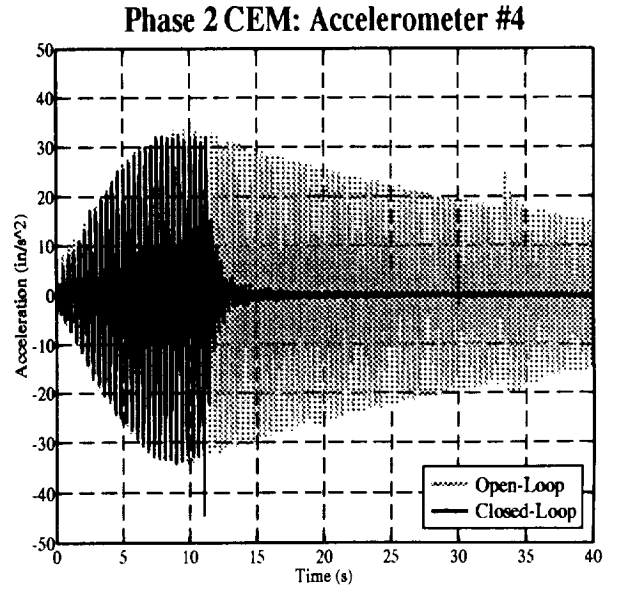
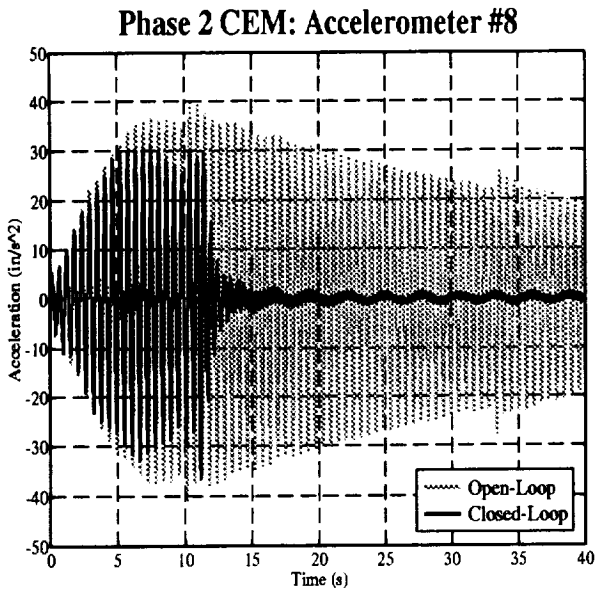


Figure 8. State Feedback Test 11: Closed-Loop versus Open-Loop Time Response

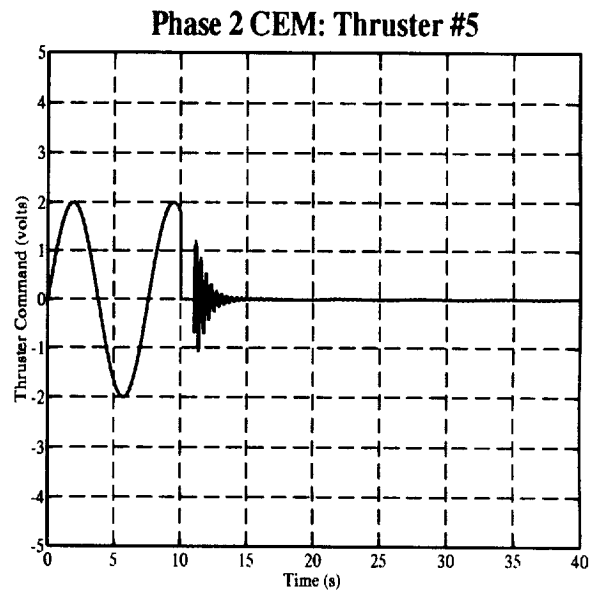
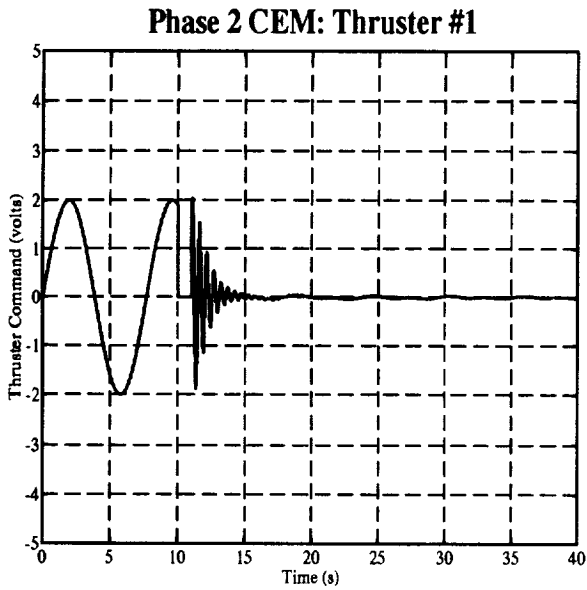
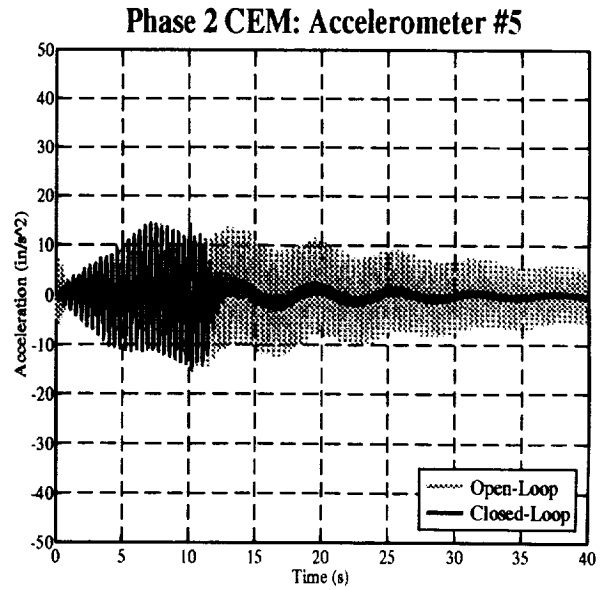
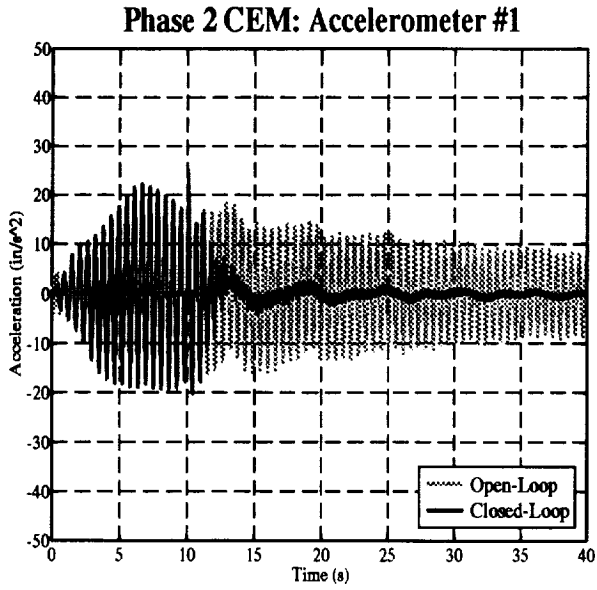


Figure 9. State Feedback Test 13: Closed-Loop versus Open-Loop Time Response (Accelerometer/Thruster Pairs 1&5)

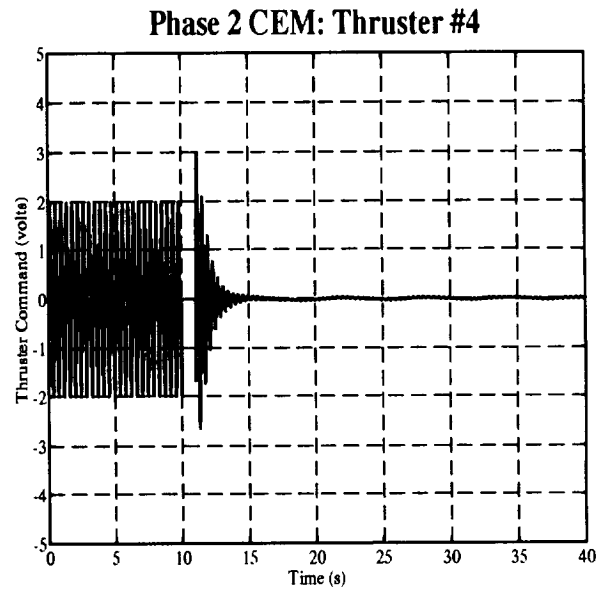
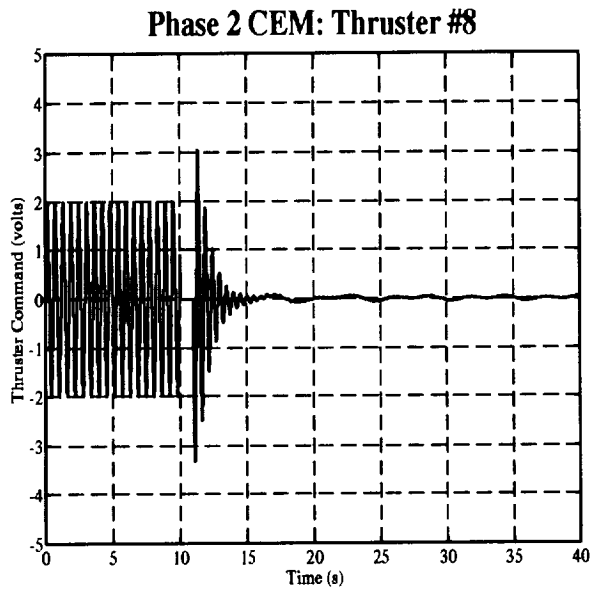
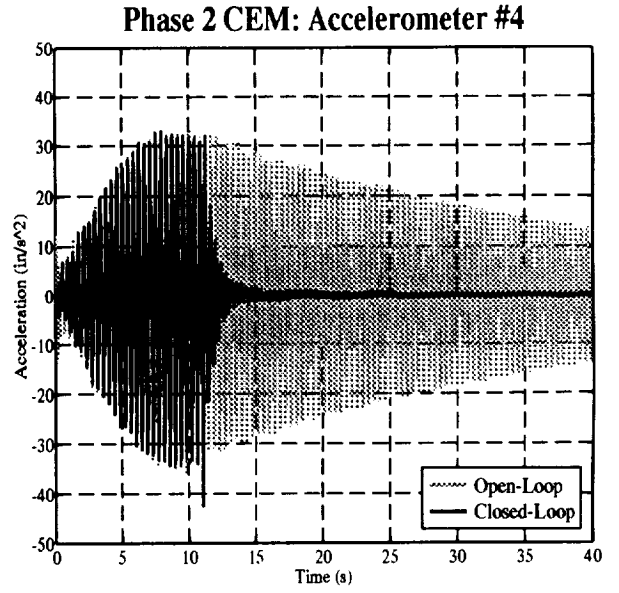
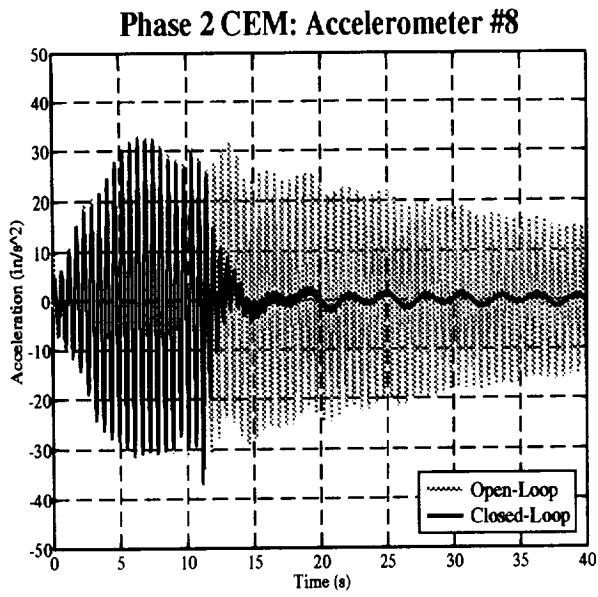


Figure 10. State Feedback Test 13: Closed-Loop versus Open-Loop Time Response (Accelerometer/Thruster Pairs 8&4)

3.5. Discussion of Results

In general the EEA controllers adequately performed their function. All the resulting closed-loop systems remained stable even in Test 13 where additional modes were excited. However in comparing the desired damping for a given mode with the measured damping shown in Table 2, one can see a noticeable difference. The difference ranges from 0.4% to 44.8% for both modes. A small part of this error can be attributed to sensor noise, measurement error, unmodeled actuator dynamics, and nonlinear dynamics of the Phase 2 structure. It was determined by the ERA/DC analysis that a majority of the error in the produced closed-loop damping was due to errors in the state space model of the Phase 2 CEM.

The state space model was created with the assumption that all modes of vibration had a damping of 0.1%. As described at the end of Section 3.3, the vibrational frequencies were derived from an eigensolution of a MSC/NASTRAN model of the Phase 2 structure. ERA/DC analysis of the open-loop test (Test 1) on the structure provided the actual values for these modal parameters. Table 3 shows that there were inaccuracies in both the assumed damping and the vibrational frequencies. Because Test 1 only substantially excited modes seven and eight, only these modes can be confidently compared with the state space model. The lack of confidence in the ERA/DC analysis of the other modes is due to high signal-to-noise ratios present in the data obtained for the other modes.

Table 3. Phase 2 CEM – Measured and Modeled Open-Loop Modes of Vibration

Source	Mode	Frequency (Hz)	Damping (%)
Actual Measured Modes	7	1.767	0.238
	8	2.432	0.178
MSC/NASTRAN State Space Model	7	1.707	0.100
	8	2.378	0.100

There is a difference of 3.4% and 2.2% in the actual and modeled frequency values of modes seven and eight, respectively, and a difference of 58% and 44% in the actual and modeled damping values of modes seven and eight, respectively. The incorrect modal parameters translate into a state space model with incorrect eigenvalues for modes seven and eight. This in turn affected the eigenvalue assignment program. The eigenvalue assignment program, using the incorrect state space model, calculated the state feedback gain matrix that would move the eigenvalues of modes seven and eight to new locations that would change the damping in those modes to a desired value. Since the model's eigenvalues were not the correct eigenvalues of the structure, when this state feedback gain matrix was applied to the actual structure the eigenvalues were moved to different locations producing damping values different from those desired. The state feedback gain matrix was calculated for the model but applied to the structure. Therefore, since the open-loop eigenvalues of the model were different from the eigenvalues of the structure, the resulting closed-loop eigenvalue for the model and the structure would be different using the same calculated feedback gain matrix. The closed-loop eigenvalues of the model produce the desired damping, but the closed-loop eigenvalues of the structure provided some other damping values.

We can determine what effect a feedback gain matrix designed for an erroneous model will have on the eigenvalues of the structure by applying that gain matrix to a corrected model. Using the results from Test 1 in Table 2, a corrected state space model of the Phase 2 structure was constructed using the measured modal parameters for modes seven and eight. The gain matrices designed for the erroneous model were applied to the corrected model, and the closed-loop eigenvalues were calculated. The damping ratios were determined from these eigenvalues, and Table 4 shows the effect of the modeling errors, detailed in Table 3, on the desired damping.

Table 4. Phase 2 CEM – Effect of Modeling Errors on Desired Damping using State Feedback

Test	Desired Damping of Mode (%)		Damping Produced from Corrected Model for Mode (%)	
	7	8	7	8
2	1.000	1.000	1.110	1.060
3	1.500	1.500	1.590	1.550
4	2.000	2.000	2.080	2.040
5	3.000	3.000	3.040	3.020
6	4.000	4.000	4.010	3.990
7	6.000	6.000	5.940	5.950
8	8.000	8.000	7.870	7.910
9	10.000	10.000	9.810	9.860
10	12.000	12.000	11.740	11.820
11	15.000	15.000	14.640	14.750

In addition to the modeling errors causing discrepancies in the eigenvalue assignment routine, they also caused errors in the Phase 2 CEM test procedure. In Section 3.4 it was described that during the first 10 seconds of a test, the structure was given an open-loop sinusoidal excitation. This was accomplished by commanding air thrusters 8 and 4 to fire at frequencies of 1.7074 Hz and 2.3782 Hz, respectively. The hope was to excite the structure at the seventh and eighth natural frequencies. The thruster frequencies were chosen to match the seventh and eighth natural frequencies of the structure according to the state space model. As was pointed out earlier, the modal frequencies of the state space model for these modes were found to be incorrect. The actual natural frequencies of the Phase 2 structure were 1.767 Hz for mode seven and 2.432 Hz for mode eight.

The slightly out of phase excitation of the structure during the controller tests produced a “beating” effect. This can be seen in the time response graphs of Figures 5-10 as a rounding off of the amplitude during the first 10 seconds. To present the effect

more clearly, Figure 11 shows a MATLAB simulation of what an open-loop excitation lasting 40 seconds would look like under the same conditions. Had the structure been properly excited at the natural frequencies, a standard open-loop time response would have looked like the MATLAB simulation depicted in Figure 12.

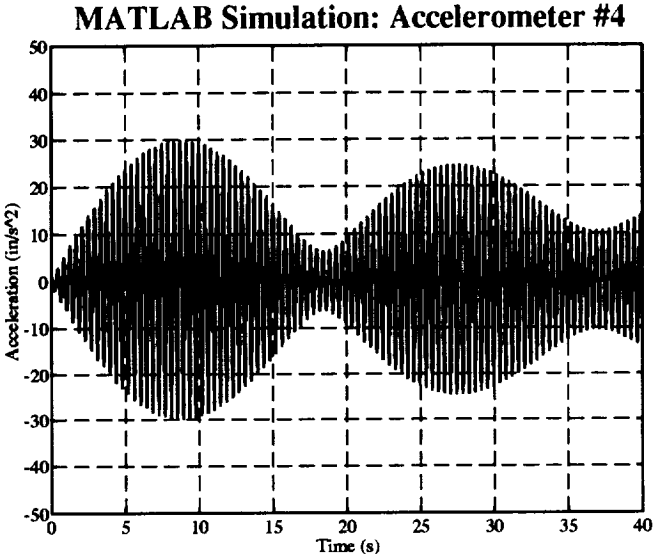


Figure 11. 40 Second Open-Loop Out-of-Phase Excitation of Phase 2 CEM

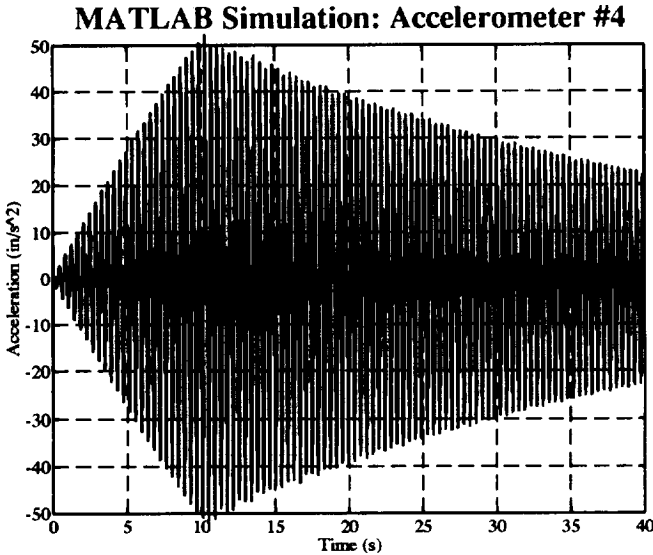


Figure 12. 10 Second Open-Loop Excitation of Phase 2 CEM at Correct Natural Frequencies

The previous paragraphs have described how errors in the state space model of Phase 2 CEM affected the performance of the eigenvalue assignment controllers. In order to show that the interaction between the structure and the controllers is now well understood, the complete test procedure was simulated in MATLAB. The simulation incorporated the actual discrete time controllers used on the structure along with a corrected state space model of the Phase 2 structure that contained the measured modal parameters for modes seven and eight. Also in the simulation, the excitation was conducted with the incorrect frequencies of modes seven and eight. Figures 13 and 14 present comparisons of the MATLAB simulation with Phase 2 CEM test data for tests 1 and 11, respectively. These figures are representative of the extremely close correlation between the time histories of the simulations and those of the actual tests on the structure.

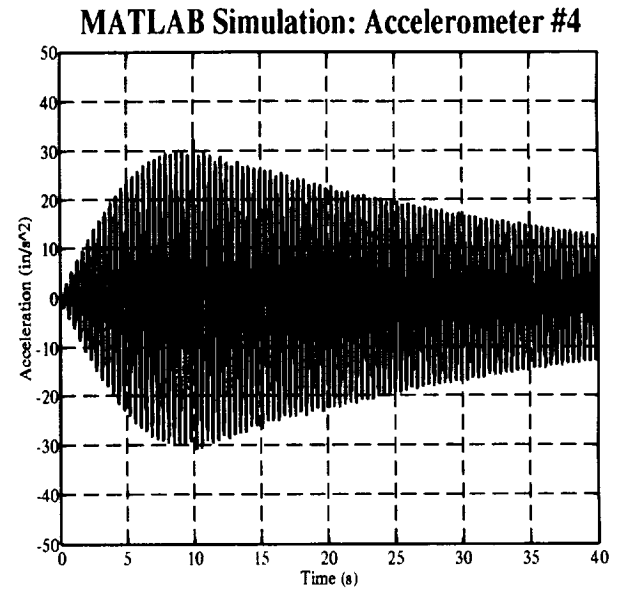
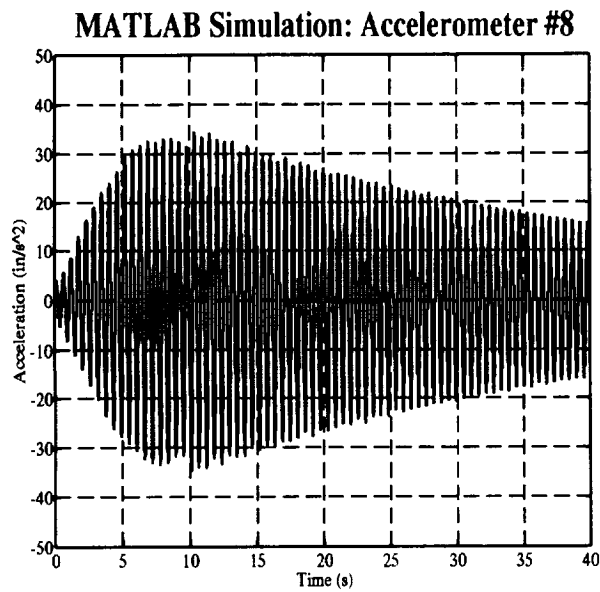
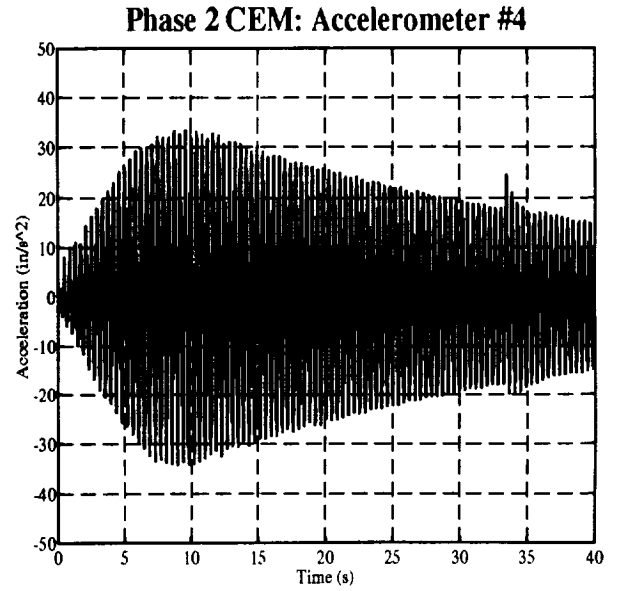
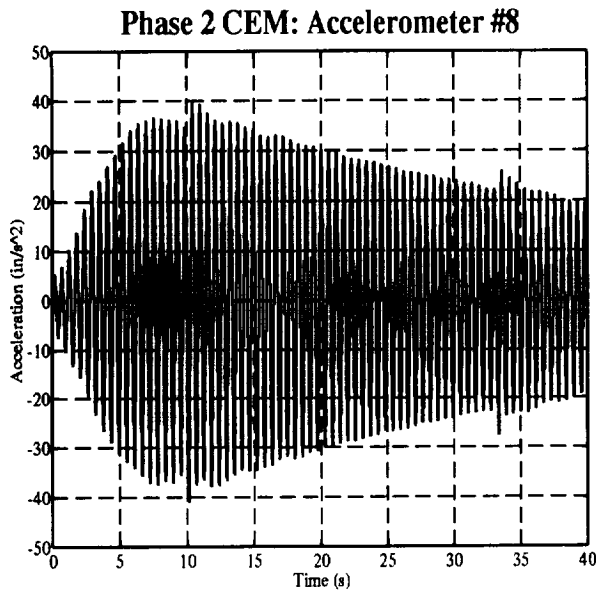


Figure 13. Time Response Comparison of Phase 2
CEM Test 1 with MATLAB Simulation of Test 1

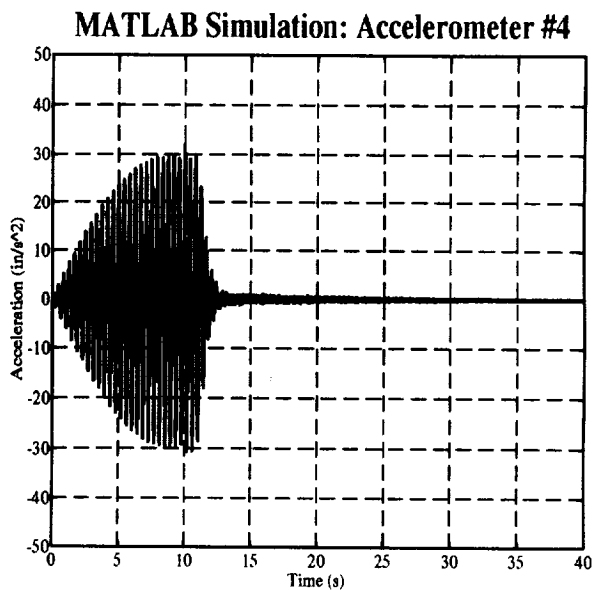
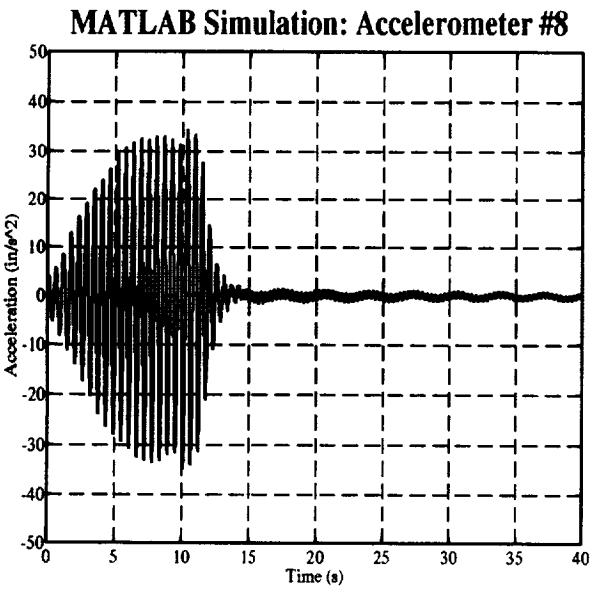
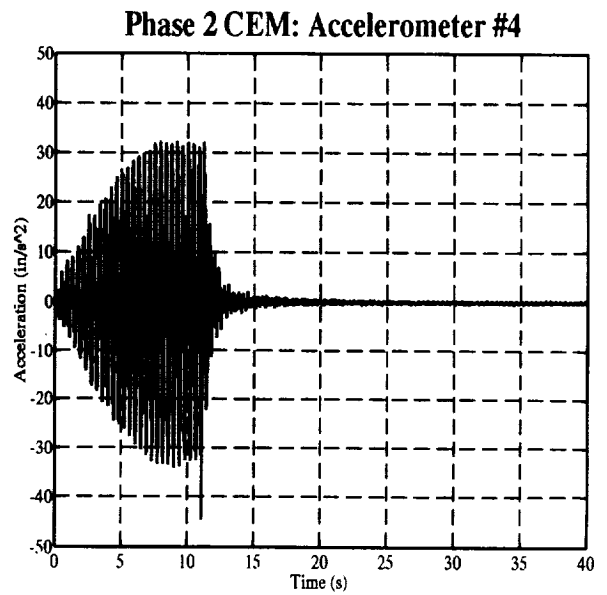
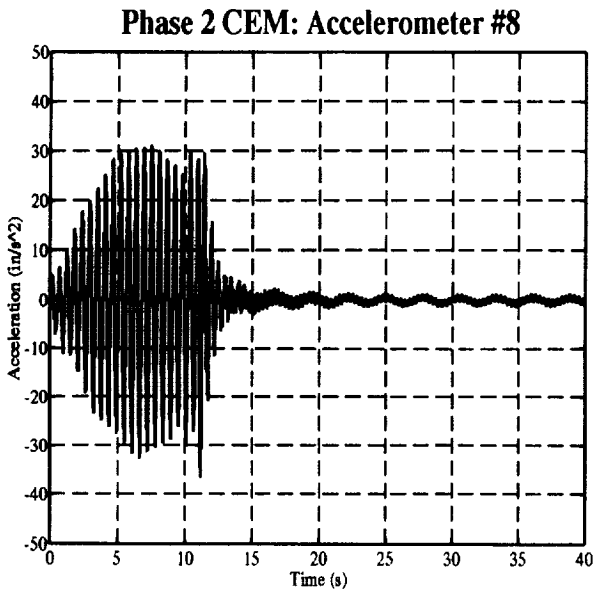


Figure 14. Time Response Comparison of Phase 2 CEM Test 11 with MATLAB Simulation of Test 11

4. SIMULATION OF OPTIMIZED OUTPUT FEEDBACK EFFICIENT EIGENVALUE ASSIGNMENT CONTROLLER ON PHASE 2 CEM

A series of controllers based on the optimized output feedback EEA algorithm were designed for the Phase 2 CEM. Disassembly of the Phase 2 CEM prevented these controllers from being tested on the structure. In order to verify the controller design software based on the optimized output feedback algorithm, these controllers were simulated on the state space model of Phase 2 using MATLAB.

4.1. Controller Design

As described earlier the output feedback EEA algorithm based directly on Maghami and Juang [8] was programmed in MATLAB. This version did not supply stabilizing controllers for the Phase 2 CEM. Therefore, the optimized output feedback algorithm was programmed in MATLAB for use as a viable controller design tool. This program makes use of the constrained nonlinear optimizer function called CONSTR supplied in the MATLAB Optimization Toolbox [33].

The optimized output feedback program requires the user to supply the system state, input, and output matrices, to specify which open-loop eigenvalues are to be kept unchanged during feedback, and to supply the desired closed-loop eigenvalues. The program then computes the output feedback gain matrix such that the resulting closed-loop system has the desired eigenvalues without affecting the prescribed open-loop eigenvalues. Using the MATLAB optimizer, the program seeks to minimize the Frobenius norm of the resulting gain matrix while attempting to stabilize the closed-loop system.

The limitations of output feedback restrict the number of eigenvalues that can be assigned. Phase 2 has eight input thrusters and eight output accelerometers. Therefore, the maximum number of eigenvalues that can be assigned is $(m + p - 1)$ or 15 or seven

pairs of eigenvalues. This number includes the number of eigenvalues held to the open-loop positions. The number of eigenvalues that can be held fixed must be less than or equal to $(m - 1)$ or 7 or three pairs. This means that up to four pairs of eigenvalues can be assigned new closed-loop values. However, just as with the controllers designed using the state feedback program, the output feedback controllers were designed to increase the damping of modes seven and eight in the Phase 2 structure. So the program was supplied with only two pairs of desired closed-loop eigenvalues. The program was also prompted to hold the eigenvalues pertaining to modes three, four, and five fixed. These particular eigenvalues were chosen through trial and error to produce the best closed-loop system performance.

4.2. Simulation Results

Three different controllers were designed and simulated. The first increased the damping of modes seven and eight to 1%, the second increased the damping to 4%, and the third increased the damping to 10%. The controllers were designed using a corrected 20 mode model of the Phase 2 structure that contained the measured modal parameters for modes seven and eight obtained from Test 1 in Table 2. The simulation conducted with these three controllers incorporated the complete test procedure carried out on the actual Phase 2 structure (see Section 3.4). This is the same simulated test procedure described at the end of Section 3.5. The controllers were simulated on a corrected 95 mode model of the Phase 2 structure.

The results of the simulations are shown in Table 5 and Figures 15-17. Table 5 compares the first ten open-loop eigenvalues of Phases 2 with the closed-loop eigenvalues of each output feedback controlled system. Note that the eigenvalues for modes three, four, and five remain at the open-loop values. The closed-loop eigenvalues for modes

seven and eight reflect an increase in damping without a change in the natural frequencies. Any deviation from this specific assignment was due to a roll-off filter that was placed in series with the controller. The roll-off filter prevents the controller from affecting the higher modes of the structure. The type of roll-off filter used in these simulations was a first-order Butterworth analog lowpass filter, created using the BUTTAP function in the MATLAB Signal Processing Toolbox [34], with a filter cut-off frequency set at 6.3 Hz. The remaining eigenvalues were free to be repositioned based on the constraints of the optimization.

Table 5. Optimized Output Feedback: Open-Loop and Closed-Loop Eigenvalues

Mode	Open-Loop Eigenvalues	Closed-Loop Eigenvalues		
		Assigned 1% Damping on Modes 7 and 8	Assigned 4% Damping on Modes 7 and 8	Assigned 10% Damping on Modes 7 and 8
1	$-0.0008 \pm 0.8180i$	$-0.0486 \pm 0.8155i$	$-0.0007 \pm 0.8224i$	$-0.1562 \pm 0.7996i$
2	$-0.0008 \pm 0.8301i$	$-0.0024 \pm 0.8297i$	$-0.0048 \pm 0.8348i$	$-0.0181 \pm 0.8266i$
3	$-0.0009 \pm 0.8565i$	$-0.0009 \pm 0.8565i$	$-0.0009 \pm 0.8565i$	$-0.0009 \pm 0.8565i$
4	$-0.0011 \pm 1.1308i$	$-0.0011 \pm 1.1308i$	$-0.0011 \pm 1.1308i$	$-0.0011 \pm 1.1308i$
5	$-0.0011 \pm 1.1401i$	$-0.0011 \pm 1.1401i$	$-0.0011 \pm 1.1401i$	$-0.0011 \pm 1.1401i$
6	$-0.0019 \pm 1.9100i$	$-0.0004 \pm 1.9162i$	$-0.0028 \pm 1.8899i$	$-0.6275 \pm 1.8604i$
7	$-0.0266 \pm 11.1024i$	$-0.1053 \pm 11.1239i$	$-0.4210 \pm 11.2065i$	$-1.1014 \pm 11.2964i$
8	$-0.0275 \pm 15.2807i$	$-0.1374 \pm 15.3223i$	$-0.5473 \pm 15.4740i$	$-1.4648 \pm 15.6857i$
9	$-0.0187 \pm 18.6919i$	$-0.1669 \pm 18.7581i$	$-0.0131 \pm 18.6878i$	$-0.4167 \pm 18.7954i$
10	$-0.0341 \pm 34.0618i$	$-0.0281 \pm 34.0567i$	$-0.0141 \pm 34.0455i$	$-0.0078 \pm 34.0481i$

Figures 15-17 show the simulated time responses for each closed-loop system compared to an open-loop system undergoing the same initial excitations. The two plots in each figure show the simulated acceleration at sensor/thruster locations 8 and 4. The acceleration responses can be easily compared with the data from state feedback tests. As with the state feedback time response plots, only data for two sensor/thruster locations are show for clarity and brevity.

One can see in the acceleration time response plots, that low frequency oscillations are present in the closed-loop system. These oscillations are in the 0.130 to 0.140 Hz range, which identifies them as being related to the first three rigid body modes of vibration. The high frequency oscillations in these plots are damped out, verifying that the controller is functioning as designed. The continued low frequency oscillations are due to a coupling between the controlled modes (modes seven and eight) and the rigid body modes that was not present in the open-loop system. Although the response of accelerometer #8 in Figure 16 may not appear to damp out during the first 30 seconds of the closed-loop simulation, the closed-loop eigenvalues for the three rigid body modes were stable. It should be noted that a controller with these characteristics may not be viable for a real spacecraft application, but it was sufficient for the purpose of demonstrating the optimized output feedback algorithm.

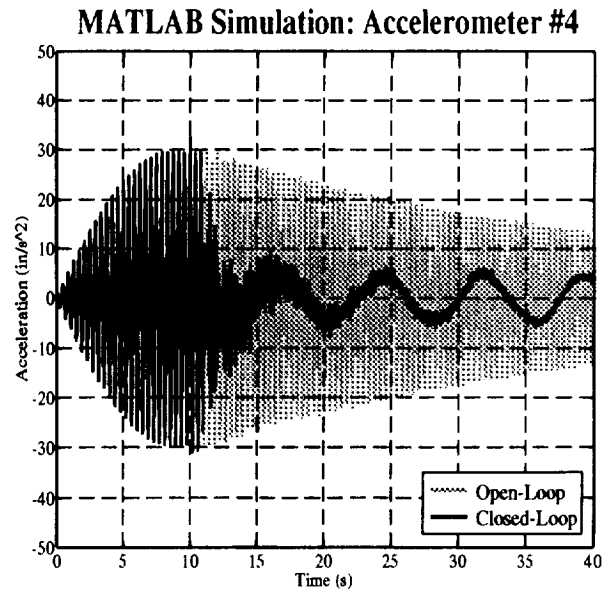
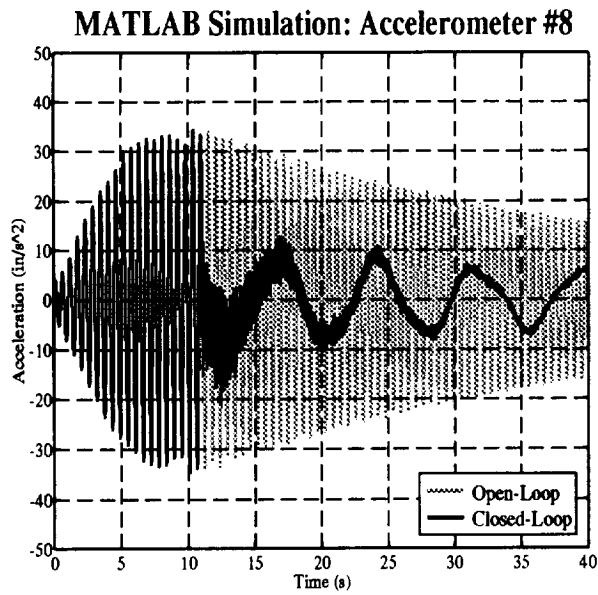


Figure 15. Output Feedback Simulation: Closed-Loop
1% Damping versus Open-Loop Time Response

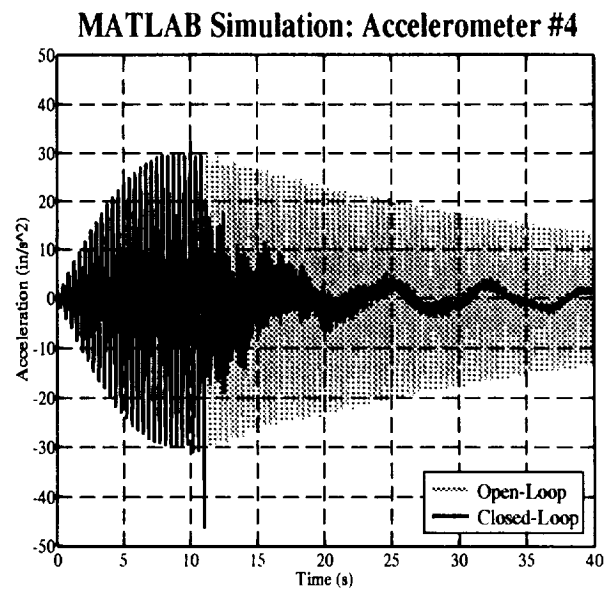
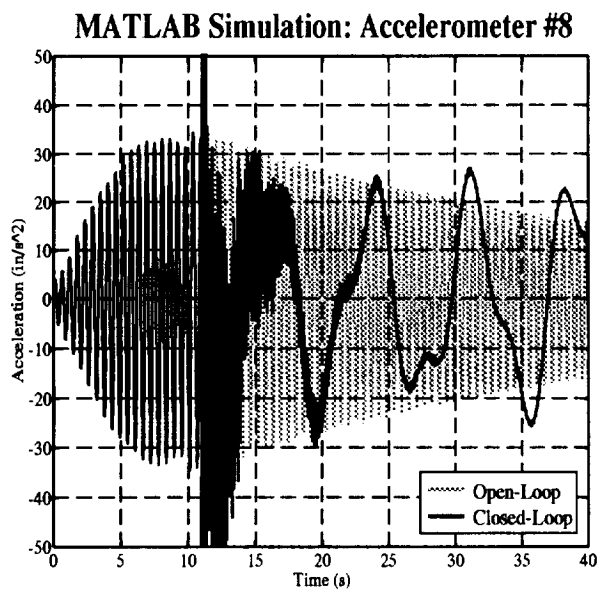


Figure 16. Output Feedback Simulation: Closed-Loop
4% Damping versus Open-Loop Time Response

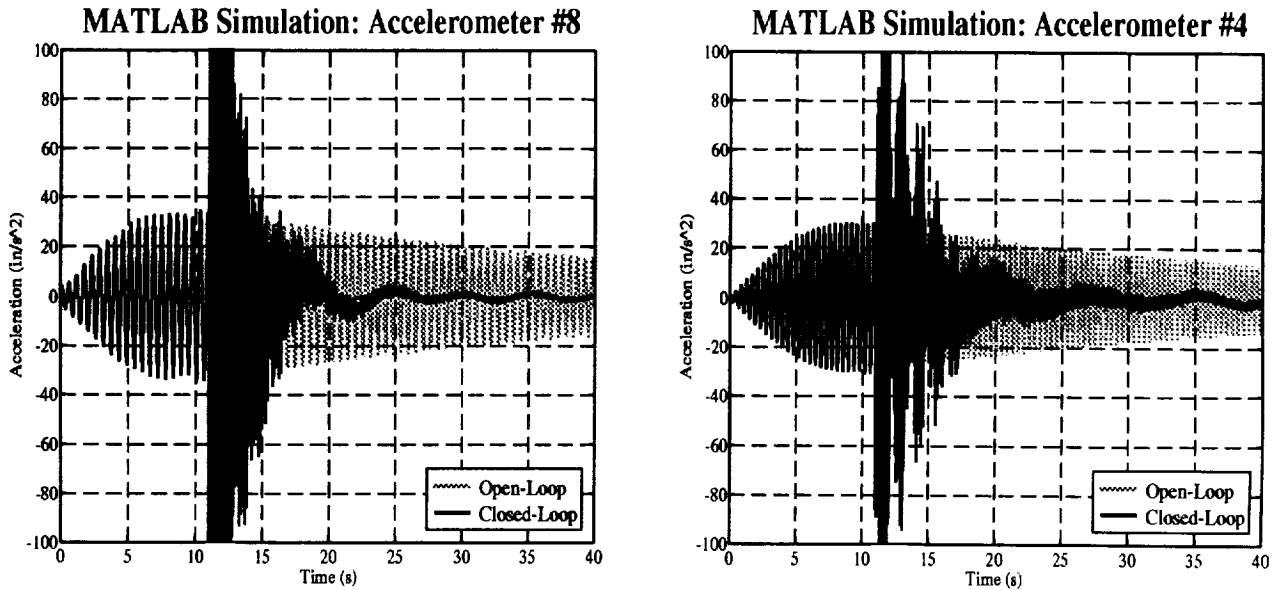


Figure 17. Output Feedback Simulation: Closed-Loop
10% Damping versus Open-Loop Time Response

It must be noted that the optimized output feedback program is very sensitive to the initial condition chosen for the coefficients c_k (see Eq. (2.25)). Different initial c_k vectors produce different feedback gain matrices after optimization is complete. Although the optimization continues until the closed-loop stability constraints are met, the optimization does not necessarily return the feedback gain matrix with the overall minimum Frobenius norm. Instead the optimization finds the local minima. This is a typical optimization result when using gradient-based optimization algorithms on non-convex problems. An alternate optimization algorithm, one that does not require gradients of the objective and constraint functions, may have provided better results, but was beyond the scope of this work. As for choosing the initial c_k vector, a routine was developed to calculate c_k from the state feedback gain matrix that assigns the same eigenvalues.

5. CONCLUSIONS

Three computer programs based on the EEA algorithms of Maghami and Juang [8] have been developed in this paper. One program is the application of the full-state feedback algorithm, a second is the application of the output feedback algorithm presented in [8], and the third is an enhancement of the second program that includes an optimization routine which chooses the feedback gain matrix such that the resulting closed-loop system is stable. All three of these programs were written in MATLAB script language and comprise the MATLAB EEA Toolbox.

Each of these three programs was used to design a series of controllers for the Phase 2 CEM. In all cases the controllers were designed to increase the damping in the seventh and eighth modes of vibration of the structure. However due to time constraints, only the state feedback controllers were tested on the actual Phase 2 CEM. The controllers based on Maghami and Juang's EEA algorithm for output feedback did not provide stabilizing controllers in simulation and, therefore, were not tested on the structure. The optimized output feedback program did provide stabilizing controllers but was not tested on the Phase 2 CEM because the structure was disassembled prior to completion of the optimized output feedback program.

Experimental validation of the state feedback assignment algorithm and program has been presented in the paper. The state feedback controllers performed as designed and placed the desired eigenvalues to new locations without affecting the remaining eigenvalues. Discrepancies between the achieved structural damping and the desired structural damping were explained and linked to modeling errors. Furthermore, as a consequence of testing the state feedback controllers on the Phase 2 structure, there was also an experimental validation of the Kalman filter as a state estimator.

The optimized output feedback program has been verified through the use of computer simulations. A series of optimized output feedback controllers were simulated in closed-loop with a computer model of the Phase 2 CEM. In each design case an output feedback gain matrix was calculated by the program to assign the desired eigenvalues while minimizing the Frobenius norm of the gain matrix and, most importantly, producing a stable closed-loop system. The simulations confirmed that the controllers did properly increase the damping of modes seven and eight. However, the closed-loop time response for each case did contain some continued low frequency oscillations after the higher frequencies were damped out. Because output feedback in general limits the number of modes that can be controlled, controllers could not be designed using the optimized output feedback eigenvalue assignment method to provide better damping for those low frequency modes.

It has been shown that the EEA algorithms using full-state feedback and optimized output feedback can be used as viable control design tools. Furthermore, the MATLAB programs of the EEA Toolbox can be easily used as numerically reliable control design software.

References

- [1] Wonham, W. M., "On Pole Assignment in Multi-Input, Controllable Linear Systems," *IEEE Transactions on Automatic Control*, Vol. AC-12, No. 6, 1967, pp. 660-665.
- [2] Moore, B. C., "On the Flexibility Offered by State Feedback in Multivariable Systems Beyond Closed Loop Eigenvalue Assignment," *IEEE Transactions on Automatic Control*, Vol. AC-21, 1976, pp. 689-692.
- [3] Davison, E. J., and Wang, H., "On Pole Assignment in Linear Systems Using Output Feedback," *IEEE Transactions on Automatic Control*, Vol. AC-20, No. 4, 1975, pp. 516-518.
- [4] Srinathkumar, S., "Eigenvalue/Eigenvector Assignment Using Output Feedback," *IEEE Transactions on Automatic Control*, Vol. AC-23, No. 1, 1978, pp. 79-81.
- [5] Chen, C. T., *Linear System Theory and Design*, Holt, Rinehart and Winston, New York, NY, 1984.
- [6] Golub, G. H., and VanLoan, C. F., *Matrix Computations-Second Edition*, John Hopkins University Press, Baltimore, MD, 1989.
- [7] Varga, A., "A Schur Method for Pole Assignment," *IEEE Transactions on Automatic Control*, Vol. AC-26, No. 2, 1981, pp. 517-519.
- [8] Maghami, P. G., and Juang, J.-N., "Efficient Eigenvalue Assignment for Large Space Structures," *Journal of Guidance, Control, and Dynamics*, Vol. 13, No. 6, 1990, pp. 1033-1039.
- [9] Petkov, P. Hr., Christov, N. D., and Konstantinov, M. M., "A Computational Algorithm for Pole Assignment of Linear Single-Input Systems," *IEEE Transactions on Automatic Control*, Vol. AC-29, No. 11, 1984, pp. 1045-1048.
- [10] Petkov, P. Hr., Christov, N. D., and Konstantinov, M. M., "A Computational Algorithm for Pole Assignment of Linear Multiinput Systems," *IEEE Transactions on Automatic Control*, Vol. AC-31, No. 11, 1986, pp. 1044-1047.
- [11] Patel, R. V., and Misra, P., "Numerical Algorithms for Eigenvalue Assignment by State Feedback," *Proceedings of the IEEE*, Vol. 72, No. 12, 1984, pp. 1755-1764.
- [12] Patel, R. V., and Misra, P., "A Numerical Algorithm for Eigenvalue Assignment by Output Feedback," *Computational and Combinatorial Methods in Systems Theory*, edited by C. I. Byrnes and A. Lindquist, Elsevier Science Publishers B. V., North-Holland, 1986, pp. 37-50.
- [13] Datta, B. N., "An Algorithm to Assign Eigenvalues in a Hessenberg Matrix: Single Input Case," *IEEE Transactions on Automatic Control*, Vol. AC-32, No. 5, 1987, pp. 414-417.

- [14] Arnold, M., and Datta, B. N., "An Algorithm for the Multiinput Eigenvalue Assignment Problem," *IEEE Transactions on Automatic Control*, Vol. 35, No. 10, 1990, pp. 1149–1152.
- [15] Kautsky, J., Nichols, N. K., and VanDooren, P., "Robust Pole Assignment in Linear State Feedback," *International Journal of Control*, Vol. 41, No. 5, 1985, pp. 1129–1155.
- [16] Bhattacharyya, S. P., and DeSouza, E., "Pole Assignment via Sylvester's Equation," *Systems and Controls Letters*, Vol. 1, No. 4, 1982, pp. 261–263.
- [17] Shafai, B., and Bhattacharyya, S. P., "An Algorithm for Pole Assignment in High Order Multivariable Systems," *IEEE Transactions on Automatic Control*, Vol. 33, No. 9, 1988, pp. 870–876.
- [18] Fahmy, M. M., and O'Reilly, J., "On Eigenstructure Assignment in Linear Multivariable Systems," *IEEE Transactions on Automatic Control*, Vol. AC-27, No. 3, 1982, pp. 690–693.
- [19] Fahmy, M. M., and O'Reilly, J., "Eigenstructure Assignment in Linear Multivariable Systems-A Parametric Solution," *IEEE Transactions on Automatic Control*, Vol. AC-28, No. 10, 1983, pp. 990–994.
- [20] Tsui, C.-C., "An Algorithm for Computing State Feedback in Multiinput Linear Systems," *IEEE Transactions on Automatic Control*, Vol. AC-31, No. 3, 1986, pp. 243–246.
- [21] Kwon, B.-H., and Youn, M.-J., "Eigenvalue-Generalized Eigenvector Assignment by Output Feedback," *IEEE Transactions on Automatic Control*, Vol. AC-32, No. 5, 1987, pp. 417–421.
- [22] Juang, J.-N., Lim, K. B., and Junkins, J. L., "Robust Eigensystem Assignment for Flexible Structures," *Journal of Guidance, Control, and Dynamics*, Vol. 12, No. 3, 1989, pp. 381–387.
- [23] Juang, J.-N., and Maghami, P. G., "Robust Eigensystem Assignment for Second-Order Dynamic Systems," *Mechanics and Control of Large Flexible Structures*, edited by J. L. Junkins, Vol. 129, Progress in Astronautics and Aeronautics, AIAA, Washington, DC, 1990, pp. 373–388.
- [24] Juang, J.-N., and Maghami, P. G., "Robust Eigensystem Assignment for State Estimators Using Second-Order Models," *Journal of Guidance, Control, and Dynamics*, Vol. 15, No. 4, 1992, pp. 920–927.
- [25] Maghami, P. G., Juang, J.-N., and Lim, K. B., "Eigensystem Assignment with Output Feedback," *Journal of Guidance, Control, and Dynamics*, Vol. 15, No. 2, 1992, pp. 531–536.
- [26] Lu, J., Chiang, H.-D., and Thorp, J. S., "Partial Eigenstructure Assignment and its Applications to Large Scale Systems," *IEEE Transactions on Automatic Control*, Vol. 36, No. 3, 1991, pp. 340–347.

- [27] Syrmos, V. L., and Lewis, F. L., "Output Feedback Eigenstructure Assignment Using Two Sylvester Equations," *IEEE Transactions on Automatic Control*, Vol. 38, No. 3, 1993, pp. 495-499.
- [28] MATLAB, Version 4.2, The MathWorks Inc., March 29, 1994.
- [29] Bryson, A. E., Jr., and Ho, Y.-C., *Applied Optimal Control*, Hemisphere Publishing Corp., New York, NY, 1975.
- [30] Newsom, J. R., Layman, W. E., Waite, H. B., and Hatduk, R. J., *The NASA Controls-Structures Interaction Technology Program*, NASA TM-102752, 1990.
- [31] MATLAB Control System Toolbox, Version 3.0b, The MathWorks Inc., March 3, 1993.
- [32] Juang, J.-N., Cooper, J. E., and Wright J. R., "An Eigensystem Realization Algorithm Using Data Correlation (ERA/DC) for Modal Parameter Identification," *Control Theory and Advanced Technology*, Vol. 4, No. 1, 1988, pp. 5-14.
- [33] MATLAB Optimization Toolbox, Version 1.0d, The MathWorks Inc., March 1, 1994.
- [34] MATLAB Signal Processing Toolbox, Version 3.0b, The MathWorks Inc., January 10, 1994.

REPORT DOCUMENTATION PAGE

Form Approved
OMB No. 0704-0188

Public reporting burden for this collection of information is estimated to average 1 hour per response, including the time for reviewing instructions, searching existing data sources, gathering and maintaining the data needed, and completing and reviewing the collection of information. Send comments regarding this burden estimate or any other aspect of this collection of information, including suggestions for reducing this burden, to Washington Headquarters Services, Directorate for Information Operations and Reports, 1215 Jefferson Davis Highway, Suite 1204, Arlington, VA 22202-4302, and to the Office of Management and Budget, Paperwork Reduction Project (0704-0188), Washington, DC 20503.

1. AGENCY USE ONLY (Leave blank)		2. REPORT DATE March 1995	3. REPORT TYPE AND DATES COVERED Technical Memorandum	
4. TITLE AND SUBTITLE Efficient Eigenvalue Assignment by State and Output Feedback with Applications for Large Space Structures			5. FUNDING NUMBERS WU 233-01-01-03	
6. AUTHOR(S) Eric C. Vannell, Sean P. Kenny, and Peiman G. Maghami				
7. PERFORMING ORGANIZATION NAME(S) AND ADDRESS(ES) NASA Langley Research Center Hampton, VA 23681-0001			8. PERFORMING ORGANIZATION REPORT NUMBER	
9. SPONSORING / MONITORING AGENCY NAME(S) AND ADDRESS(ES) National Aeronautics and Space Administration Washington, DC 20546-0001			10. SPONSORING / MONITORING AGENCY REPORT NUMBER NASA TM-110155	
11. SUPPLEMENTARY NOTES Vannell: George Washington University (JIAFS program), Hampton, VA				
12a. DISTRIBUTION / AVAILABILITY STATEMENT Unclassified-Unlimited Subject Category 18			12b. DISTRIBUTION CODE	
13. ABSTRACT (Maximum 200 words) The erection and deployment of large flexible structures having thousands of degrees of freedom require controllers based on new techniques of eigenvalue assignment that are computationally stable and more efficient. Scientists at NASA Langley Research Center have developed a novel and efficient algorithm for the eigenvalue assignment of large, time-invariant systems using full-state and output feedback. The objectives of this research were to improve upon the output feedback version of this algorithm, to produce a toolbox of MATLAB functions based on the efficient eigenvalue assignment algorithm, and to experimentally verify the algorithm and software by implementing controllers designed using the MATLAB toolbox on the Phase 2 configuration of NASA Langley's Controls-Structures Interaction Evolutionary Model, a laboratory model used to study space structures. Results from laboratory tests and computer simulations show that effective controllers can be designed using software based on the efficient eigenvalue assignment algorithm.				
14. SUBJECT TERMS Eigenvalue assignment, Flexible systems, State feedback, Output feedback, Optimization			15. NUMBER OF PAGES 69	
			16. PRICE CODE A04	
17. SECURITY CLASSIFICATION OF REPORT Unclassified	18. SECURITY CLASSIFICATION OF THIS PAGE Unclassified	19. SECURITY CLASSIFICATION OF ABSTRACT	20. LIMITATION OF ABSTRACT	